UNIVERSITY OF ÇUKUROVA
INSTITUTE OF NATURAL AND
APPLIED SCIENCES

MSc THESIS

Neveser ÇAYIRCI

INDOOR WIRELESS PROPAGATION MODELS AND MEASUREMENTS

DEPARTMENT OF ELECTRICAL AND
ELECTRONICS ENGINEERING

ADANA, 2005

ABSTRACT

MSc THESIS

INDOOR WIRELESS PROPAGATION MODELS AND MEASUREMENTS

Neveser ÇAYIRCI

DEPARTMENT OF ELECTRICAL AND ELECTRONICS ENGINEERING
INSTITUTE OF NATURAL AND APPLIED SCIENCES
UNIVERSITY OF ÇUKUROVA

Supervisor : Prof. Dr. Hamit SERBEST
Year: 2005 Pages: 54
Jury : Prof. Dr. A. Hamit SERBEST
Prof. Dr. Süleyman GÜNGÖR
Asst. Prof. Dr. Turgut İKİZ

Due to the great success of wireless communications used in outdoor mobile radio systems, the wireless communication inside vehicles and buildings becomes more and more important. There have been a number of recent investigations on indoor radio propagation modeling. In the last years different prediction models for indoor environments were developed for the frequency range between 500 MHz and upper frequencies (at GHz).

In this thesis, the most popular two models used for indoor propagation are tested and compared to one another and to measurements in various indoor environments. Indoor propagation is, of course, more complex than outdoor propagation becaused received signal strength depends on open plan offices, construction materials, building structure, density of people, furniture, etc. Various objects may scatter, diffract, reflect, and absorb radiation and cause decrease in the received level of signal level. Therefore, accurate characterization of the building materials is necessary for prediction of wave propagation behavior within indoor environments.

For this purpose, in the present work, a free-space method for the investigation of dielectric properties is used and cement-based materials (concrete) are measured at microwave frequencies for determining transmission and reflection coefficients.

Keywords :Indoor Radio Propagation, Path Loss, GTD, Free-Space Method, Dielectric Permittivity.

ÖZ

YÜKSEK LİSANS TEZİ

KAPALI YERLERDE KABLOSUZ İLETİŞİM ÖLÇÜM VE MODELLERİ

Neveser ÇAYIRCI

ÇUKUROVA ÜNİVERSİTESİ
FEN BİLİMLERİ ENSTİTÜSÜ
ELEKTRİK-ELEKTRONİK MÜHENDİSLİĞİ ANABİLİM DALI

Danışman : Prof. Dr. Hamit SERBEST
Yıl: 2005 Sayfa: 54
Jüri : Prof. Dr. A. Hamit SERBEST
Prof. Dr. Süleyman GÜNGÖR
Doç. Dr. Turgut İKİZ

Açık alan mobil radyo sisteminde kullanılan kablosuz iletişimin büyük başarısından dolayı, araç ve bina içlerindeki, kablosuz iletişimin önemi gittikçe artmaktadır. Kapalı çevre radyo yayınımı modelleme üzerine yapılmış çok sayıda araştırma mevcuttur. Son yıllarda 500 MHz ve daha yüksek frekanslar (GHz) için kapalı çevre kestirim modelleri geliştirildi.

Bu tez çalışmasında kapalı alan uygulamalarında kullanılan iki popüler model kullanılarak hesaplamalar yapıldı ve farklı kapalı alan çevreler için elde edilen ölçümler ile karşılaştırıldı. Kapalı alan yayınım, açık alan yayınımdan elbette daha komplekstir çünkü alınan sinyal gücü, binaların yapılarına, ofis planlarına, kullanılan yapı materyallerine, insan yoğunluğuna, bina içlerindeki mobilyalara ve daha benzer birçok etkilere bağlıdır. Burada saçılan, yansıyan, yutulan, kırınıma uğrayan ışınlar, alınan sinyalin seviyesinde düşüşe sebep olurlar. Bundan dolayı, kapalı alanlarda dalga yayınımının davranışını tahmin edebilmek için bina yapı karakterlerini bilmek gereklidir.

Bu amaç için, bu çalışmada dielektrik özelliklerin incelenmesi için boşluk-uzay metodu kullanıldı ve çimento tabanlı materyallerin mikro dalga frekanslarında yansıma ve kırılma katsayıları ölçüldü.

Anahtar Kelimeler :İndoor Dalga Yayınımı, Yol Kaybı, GTD, Kompleks Dielektrik Geçirgenlik, Boşluk Uzay Yöntemi .

ACKNOWLEDGEMENTS

I would like to express my gratitude to my supervisor Prof. Dr. A. Hamit SERBEST for all of his supports, guidance, suggestions, patience in this study.

I would also like to express my thanks to Prof. Dr. Süleyman GÜNGÖR, the head of the Department of Electrical and Electronics Engineering, and to Assoc. Prof. Dr. Turgut İKİZ for their supports.

I would like to express my appreciation to Assoc. Prof. Dr. Sami ARICA for his guidance, auspices and help and to S. Barbaros YABACI (Turkcell Operator) for his technical – help, and also thanks to my family for their supports.

CONTENTS **PAGE**

LIST OF TABLES PAGE

LIST OF FIGURES **PAGE**

NOTATIONS

k_s	Wave number of sample
k_1	Wave number of first medium
k_2	Wave number of second medium
r	Reflection coefficient
R	Reflection coefficient in decibel
t	Transmission coefficient
T	Transmission coefficient in decibel
t_s	Thickness of the sample
β_0	Angle between incident ray and the edge of the wedge
β	Phase constant
ε	Permittivity
ε_r	Relative permittivity
ε_o	Permittivity in vacuum
θ_i	Incident angle
θ_r	Reflected angle
θ_t	Transmitted angles
λ_o	Free-space wavelength
μ_o	Permeability of vacuum
Γ_h	Reflection coefficient for parallel polarization
Γ_v	Reflection coefficient for perpendicular polarization
T_h	Transmission coefficient for parallel polarization
T_v	Transmission coefficient for perpendicular polarization
ψ	Direction of propagation of the incident field
ψ_0	Direction of propagation of reflected fields
d_0	Reference distance (typically 1 m)
d	Distance between transmitter and receiver

k	Number of floors the signal encounters
F	Loss per floor (decibels)
ℓ	Number of walls the signal encounters
W	Loss per wall (decibels)
P	Path loss (decibels)
L	Unit loss, path loss (decibels) at 1 m from the transmitter antenna

1. INTRODUCTION

The importance of indoor radio communication systems is increasing day by day. The great success of wireless communications used in land mobile radio systems causes the wireless communication inside vehicles and buildings become more important. It is well known that the propagation of electromagnetic waves within these environments creates very complicated interactions with the building structures. The effect of the external and internal walls, floors, ceilings and windows on the electromagnetic wave modify the amplitudes and phases of the propagating signals. Therefore, characterization of the building materials is a must for predicting wave propagation correctly within indoor environments.

There are simple models to predict signal power at indoor environments. Although, these simple path loss propagation models are suitable only for unobstructed Line of Sight (LoS) communications, this is not the case in an indoor environment.

The purpose of this study is to apply the empirical model and ray tracing technique for the investigation of indoor radio propagation. Also, the theoretical signal values obtained by these methods are compared with the measurements results.

Bernardi et al (2004) proposed a model for the analysis of complex indoor radio environments, in which microwave WLAN systems operate. They showed that the electromagnetic field distribution and the channel performances are significantly influenced by the diffraction processes arising from the presence of furniture.

Chin et. al. (1998) presented a comparison of the empirical and deterministic model for indoor radio propagation. They compared results for these models and they showed that the central area of a room is heavily affected by multipath, as signals which are reflected off walls will all interfere mostly at the center point of the room.

Tam et. al. (1995) introduced two propagation models for indoor. The estimates of the signal strength that will be obtained by propagation models are useful in the design and installation of indoor radio systems. Tam et.al. classified propagation models as statistical models and site-specific propagation models and stated that while statistical models need extensive measurement data they do not provide site-specific information but site-specific propagation models provide site-specific information but require considerable detail of the layout of the indoor environment.

Vinko, et.al (1998), combined with Ray theory and the Uniform Geometrical Theory of Diffraction to characterize signal propagation characteristics in urban and suburban environments and to investigate reflection and diffraction rays along to NLOS paths. They presented and compared two different modeling approaches with experimental data. The results show excellent agreement between theory and measurements for different bands and different locations. Also, they found that the Power-of-Complex-Sum method should be used at lower frequencies, while the Sum-of-Individual-Ray-Powers method should be used at higher frequencies.

Yang et.al. (1998) presented a ray-tracing method for waves propagating inside building structures. They developed a ray-tracing program for modeling indoor wave propagation and penetration. Multiple reflections and transmissions of ray tubes inside and among walls, ceilings/floors, and other building structures are traced to determine the GO contributions. They used ray tubes to model the wave propagation and penetration and all the significantly reflected and transmitted ray tubes and gave comparison with model and measurements in building where good agreements were obtained.

The, characterization of dielectric properties of the building structure is important to understand signal behavior for indoor propagation. In microwave techniques, dielectric properties are usually derived from measurements of reflection or transmission coefficients or both. Free-space microwave techniques have been widely used for dielectric property measurements, Kharkovsky et. al. (2001), Ma and Okamura (1999). Ghodgaonkar et. al. (1989).

Ghodgaonkar et. al. (1989) developed a free-space measurement system in the frequency range of 14.5-17.5 GHz for the measurements of dielectric properties of planar slabs of ceramic and composite materials. They calculated the dielectric constants and loss tangents from the measurements of reflection coefficients by applying transmission line theory.

Ma and Okamura (1999) proposed a method to determine the permittivity of material by using only the amplitudes of the transmission and reflection coefficients. According to their analysis, the permittivity can be uniquely determined by measuring these two amplitudes when a sample is prepared with large enough attenuation that the multiple reflections between the two surfaces of the sample can be neglected.

At the department of Electrical and Electronics Engineering in Çukurova University, the measurements of reflection and transmission properties of cement-based structures by using free-space method have been conducted since 2000. The results of reflection properties of cement-based materials during all stages of hydration process and different curing conditions were presented in the report by Kharkovsky et. al. (2001). The investigations were made for a variety of typical cement-based structures with different content and dimensions at X-band (8-12 GHz). It is very interesting to use only the amplitudes of the reflection and transmission coefficients for investigation of cement-based materials, particularly for the determination of dielectric permittivity, because of such advantages of this technique as simplicity and low cost.

The thesis is organized like this, Section II introduces the methods which are used to predict for indoor radio propagation. The models are the empirical and the ray tracing technique. The total received power is estimated by using these models.

Section III describes the characteristics of the building where the measurements of signal power were made, including, the overall building structure and layout of each of the floors. Next, Section IV, discusses how the measurements were made in the building and results of measurements were compared with the empirical model and the ray tracing model.

Finally, in Appendix, a free-space method is introduced. The effective dielectric constants of the building structures are determined from a free-space method. The main features of the method are to measure only the amplitudes of transmission and reflection coefficients at microwave frequencies and to determine the relative permittivity by using a numerical method. These measurements were made with concrete specimens which have different thickness and ratio of water/cement between 8.4 GHz and 12 GHz.

2. METHODS

In this chapter, the methods that are used in this study for the investigation of indoor propagation characteristic are introduced. There are generally two methods for the investigation of radio propagation, the "Empirical model" and the "Deterministic model", (Clarke, 2002). The empirical model is very useful and easy to apply for predicting signal propagation for indoor propagation but it has several deficiencies in explaining the propagation mechanisms. The second model which is based on ray-tracing technique, is more sensitive and more explanatory but, more complex than the first model.

2.1. Empirical Model

The empirical model is based on measurements taken at different locations of the region that is to be modeled. The measurement values are then used to fit them into an approximate mathematical model named as the Path Loss model (Doble, 1996). Path loss models represent the difference (in dB) in signal strength between the transmitter and the receiver, but it does not take into account the multipath propagation.

A typical wave propagation along within the same floor with no obstructions between the transmitter and the receiver, the mean path loss in dB (PL) increases logarithmically with distance.

$$PL(d) = PL(d_0) + 10\log (d/d_0)^n$$

In the path loss expressions, the exponent n is named distance/power law coefficient and it is taken as 2 for free space, that is what, we have assumed in the present study. The reference distance which is typically 1 m in the far field of the transmitter is shown by d_0. The distance between the transmitter and receiver is d.

However, the number of walls and floors (obstacles) between the transmitter and the receiver introduce extra losses to the received signal level. The propagation prediction model can be improved by introducing, an average Wall Attenuation Factor (WAF) and a Floor Attenuation Factor (FAF) which describe the additional losses caused by walls and floors between transmitter and receiver. The mean path loss with the additional attenuation factor is then given as;

$$PL(d) = PL(d_0) + \sum_{i=0}^{N} WAF(i) + \sum_{j=0}^{M} FAF(j) + 10.\log(d/d)^n$$

Or as follows, (Doble, 1996);

$$PL(d) = L\ (\text{Unit Loss}) + n.\ 10.\ \log(d / d_0) + k.F + \ell.W$$

Here $WAF(i) = \ell.W$, $FAF(j) = k.F$ and $PL(d_0)= L$, ℓ and k denote number of walls and floors between the transmitter and receiver, respectively. On the other hand, P is the path loss in dB and L (Unit loss) is the path loss (dB) at 1 m from the transmitter antenna . The Unit Loss is calculated as $20\log(4\pi d_0/\lambda)$ and it yields 31 dB for 900 MHz.

F and W denote the losses for floor and wall, respectively, in dB and $k.F$ and ℓW give the total floor and wall attenuations, since k and ℓ are the numbers showing how many floors and walls the signal encounters.

The model can performs well in certain circumstances, but due to the approximations done at the beginning, as all methods it has some limitations. For example it doesn't include reflected, transmitted and diffracted rays and also the physical properties of the obstructions are not taken into account.

The power level received at the mobile receiver is,

$$P_{rec} = P_{trans} - P\ (\text{path loss})$$

$$P_{rec} = P_{trans} - \left(20\log\left(4\pi d_0 / \lambda\right) + 10.n.\log\left(d / d_0\right) + k.F + \ell.W\right)$$

Which combines both propagation losses within the buildings and the penetration losses. Although, such a statistical model is simple and it takes into account only the direct path between the transmitter and the receiver. It is obvious that, the path-loss depends upon the building type and environmental clutter. The simplicity of the model gives the chance to generate the results very quickly, by assuming that the reflected and diffracted rays give only minor contribution at the total field. Also it considers the path loss-distance relationship as a straight line, and WAF and FAF are chosen to be indepented from construction type of the material.

Unfortunately, this is not enough to define and explain propagation behavior of the signal in indoor case.

Because, while propagating in the buildings, radio signals pass through various materials before reaching a receiver antenna. The interaction of these radio signals with building materials usually result attenuation in the signal strength. Also, it should be noted that depending on that medium's characteristics and specific electrical properties, signals behave differently when encountering an obstructing medium. These electrical properties, which are naturally unique for every material, determine how a signal can transmit through the medium. More specifically, RF energy entering a building will be partially absorbed and partially scattered by the material components encountered in the building.

In the empirical model for floor and walls attenuation, the user must take certain constant values. The thickness and type of the walls and floors surely have an important role on the amount of attenuation that the signal encounters. Depending on type of materials used in the walls and thickness of the walls, the wall loss factor, at 900 MHz, lies in the range 0.4 dB and 29 dB. For considering losses through partitioning walls within a building, the situation is simplified and just three classifications are considered as light, medium and heavy with 1.5 dB, 5 dB and 10 dB losses, respectively (Doble, 1996).

2.2. Ray Tracing Technique

In this part, a different approach is introduced for indoor propagation which is the application of ray-tracing technique in combination with GTD (Geometrical Theory of Diffraction). Again, the power received at the receiver is given as, Prec = Ptrans – P (path loss). In this model, deterministic solution of ray theory and the Geometrical Theory of Diffraction (GTD) are combined to predict the average of signal strength for propagation through indoor environments.

The obstructions in the form of walls, roofs, furniture, people,…etc. in the buildings surely effect the propagation of the radio waves in various ways. When an electromagnetic wave impinges on an object which is larger than the signal wavelength, it will be either reflected, refracted (transmitted) or diffracted. These mechanisms in general are named as scattering and this may cause a propagating wave to loose power.

Reflection, refraction and transmission will occur when a signal is scattered by the geometrically smooth part of the surface and diffraction occurs when an electromagnetic wave is obstructed by the irregularities of the surface such as edges, corners and tips. Also, surface diffraction will occur when the ray tangentially strikes the geometrically smooth surface such cylinders or spheres. In general, all type of diffracted rays are the reasons for the illumination in the geometrically dark shadow regions. These effects lead to multiple propagation paths for one signal and so lead to the multipath effect along Line-of Sight (LOS) and Non-Line-of-Sight (NLOS) paths.

Although the accuracy of this deterministic model compared to the empirical model is a great superiority, it is computationally expensive and therefore must be simplified to enable both accurate modeling and acceptable time-effort cost.

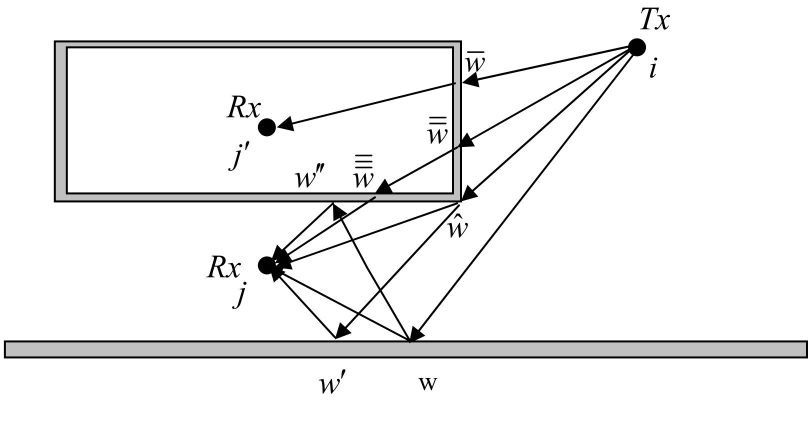

Figure 2.1. Illustration of the reflected, transmitted and diffracted rays.

To illustrate the scattering mechanism an indoor environment is shown in Figure 2.1. the transmitter is located sufficiently far away from the obstructions which are part of a wall and the walls of a room. Here, (i) denotes the location of the transmitter and the points (j) and (j') are the receiver locations for two different cases. Similarly, w, w', w'' are the reflection points, $\overline{w}$, $\overline{\overline{w}}, \overline{\overline{\overline{w}}}$ are the transmission points and $\hat{w}$ is the diffraction point.

As the ray, optical components, the reflected and transmitted rays are expressed in terms of the incident field amplitude and the reflection/transmission coefficient. The reflected field is

$$E^r(j) = E^i(w).\Gamma(w).\frac{s_{iw}}{s_{iw} + s_{wj}} e^{-jks_{wj}}$$

Here, Γ is the value of the reflection coefficient at the reflection point, *s* denotes the optical path and the first and second index are the starting end points of the ray, respectively.

The transmitted field is expressed similarly,

$$E^t(j') = E^i(\overline{w}).T(\overline{w}).\frac{s_{i\overline{w}}}{s_{i\overline{w}} + s_{\overline{w}j'}} e^{-jks_{\overline{w}j'}}$$

Where, T is the transmission coefficient.

Now, for the diffracted field, the following expression is written in the same manner.

$$E^d(j) = E^i(\hat{w}).D(\hat{w}).A(\hat{w}, j).\sqrt{\frac{s_{i\hat{w}}}{s_{\hat{w}j}.s_{i\hat{w}}}} e^{-jks_{wj}}$$

Where, D is the diffraction coefficient and E^d (j) is the value of the diffracted field at the observation point. A($\hat{w}$, j) is the coefficient describing amplitude variation along the diffracted ray. For a spherical wave incidence the attenuation factor is defined as the following:

$$A(\hat{w}, j) = \sqrt{\frac{s_j}{s_{\hat{w}}(s_j + s_{\hat{w}})}}$$

If a multiple scattering mechanism is observed as the ray propagating from (i) to (j) through ($\hat{w}$) and (w'), then it is obvious that the incident ray is first diffracted, then reflected and then observed at the receiving antenna. In this case, the resulting expression is

$$E^{d,r}(j) = E^{i}(\hat{w}).D(\hat{w}).A(\hat{w},w').\Gamma(w').\sqrt{\frac{s_{i\hat{w}}}{(s_{\hat{w}w'}+s_{w'j})(s_{i\hat{w}}+s_{\hat{w}w'}+s_{w'j})}}e^{-jks_{w'j}}$$

Another examples for multiple scattering are the transmitted-transmitted and reflected –reflected rays which are also shown in Figure 2.1.

$$E^{t,t}(j) = E^{i}(\overline{\overline{w}}).\mathrm{T}.\mathrm{T}'.\frac{s_{i\overline{\overline{w}}}}{s_{i\overline{\overline{w}}}+s_{\overline{\overline{w}}\overline{\overline{\overline{w}}}}+s_{\overline{\overline{\overline{w}}}j}}e^{-jks_{\overline{\overline{\overline{w}}}j}}$$

$$E^{r,r}(j) = E^{i}(w).\Gamma.\Gamma'.\frac{s_{iw}}{s_{iw}+s_{ww''}+s_{w''j}}e^{-jks_{w''j}}$$

Where, T' and Γ' are the transmission and reflection coefficients for 2nd reflector. w'' is the optical path length for ‘th reflected surface and $\overline{\overline{w}},\overline{\overline{\overline{w}}}$ are the optical path lengths ‘th transmitted surfaces.

There is also an additional contribution to the signal power because of the other paths by which rays can reach the receiving antenna. The paths shown in Figure2.1. are not the only possible paths that could occur due to multiple scattering. Although all of these rays make contributions to the total field at the observation point, it is not possible to take all into contribution. Therefore, multiple scattering of order higher than two are assumed to be negligible and their contributions are not taken into consideration in this study. It is useful to express multiple reflection, transmission and diffraction in a compact form and they are given below for each case separately :

$$\sum E^{r} = \sum_{x}^{N}\left[\; E^{i}(w).\prod_{x}\Gamma_{x}.\frac{s_{iw}}{s_{iw}+s_{wj}}e^{-jks_{wj}}\;\right]$$

$$\sum E^{t} = \sum_{y}^{N}\left[\; E^{i}(w).\prod_{y}\mathrm{T}_{y}.\frac{s_{iw}}{s_{iw}+s_{wj}}e^{-jks_{wj}}\;\right]$$

for diffracted field

$$\sum E^d = \sum_{z}^{N} [\ E^i(w). \prod_{z} D_z . A_z(w,j). \sqrt{\frac{s_{iw}}{s_{wj} . s_{ij}}} e^{-jks_{wj}}\ ]$$

Here, $s_{i,j,w}$ are the optical path lengths, Γ_x is the reflection coefficient for the x'th reflector, T_y is the transmission coefficient for the *y'th* surface, D_z is the diffraction coefficient of the *z'*th diffraction point, while N denotes the number of scattering.

The predicted signal level is given by the following:

$$P_p = 20\log_{10} \left[\left| E^r + E^d + E^t \right| \right]$$

and, received power can be written as,

Pr = Pt - (PL(d) + Pp), which yields Pr = Pt - (PL(d0) + 10log $(d/d_0)^2$ + Pp).

The new model combined four new features of distance dependence, reflection, transmission and diffraction. Penetration loss is introduced when signal passing through walls (or obstacle) and the signal attenuation depends on the characteristic of the walls. Diffracted rays are calculated according to Keller's Geometrical Theory of Diffraction principle.

3. STUDY AREA

The modeling and measurements for indoor propagation at 900 MHz in this study is accomplished in the Electrical and Electronics Engineering building of the University of Çukurova. The structure of the building will be introduced on floor plans and the points of investigation will also be shown.

The Electrical and Electronics Engineering at the University of Çukurova is located a at three storey building. This building with offices and laboratories may be considered as of a typical office structure. External walls are concrete, with metal screened windows, internal walls are usually air-brick made (some heavy walls also exist) and building entrance consists of glass panel door. Floors and ceilings are both in concrete and the ceilings are covered with thin metal grids. This section describes the characteristics of the building where the measurements were made. In particular, the overall building structure and layout of each of the floors is presented.

Indoor radio channels do not suffer from the environmental effects of snow, rain, hail, clouds or temperature inversion as do outdoor radio channels but because of the variation of building size, shape, structure, layout of rooms and the type of construction materials are most importantly for Indoor radio channels. The electromagnetic wave propagation inside a building is a more complex multipath structure than that of terrestrial mobile radio channels. For example, a factory building is quite different to an office building both in its structure and in the materials used. The variation of type of materials used in internal partitions, outside walls, ceilings and floors, as well as the size and, percentage of, windows, age of building, people density and activity are also factors which complicate indoor electromagnetic-wave propagation.

Measurements were taken on the ground, 1st and 2nd floors and a plan showing the locations of the 900 MHz measurements on the floors are given.

The rays from the transmitter antenna are reflected off walls, partitions, ceilings, floors and tables etc. or transmitted through walls and partitions etc. to arrive at the receiver. For LOS propagation, it is easy to trace the ray by connecting the transmitter and receiver.

Propagation losses were measured by a straight line along the corridor on one floor of the building. The variation in signal strength, was measured in LOS and NLOS conditions. The rooms contain standard laboratory equipment, several computers and black boards. The walls are made of concrete blocks considered as rough surface. The measurement points at different parts of the building are shown in Figure 3.1., 3.2. and 3.3.

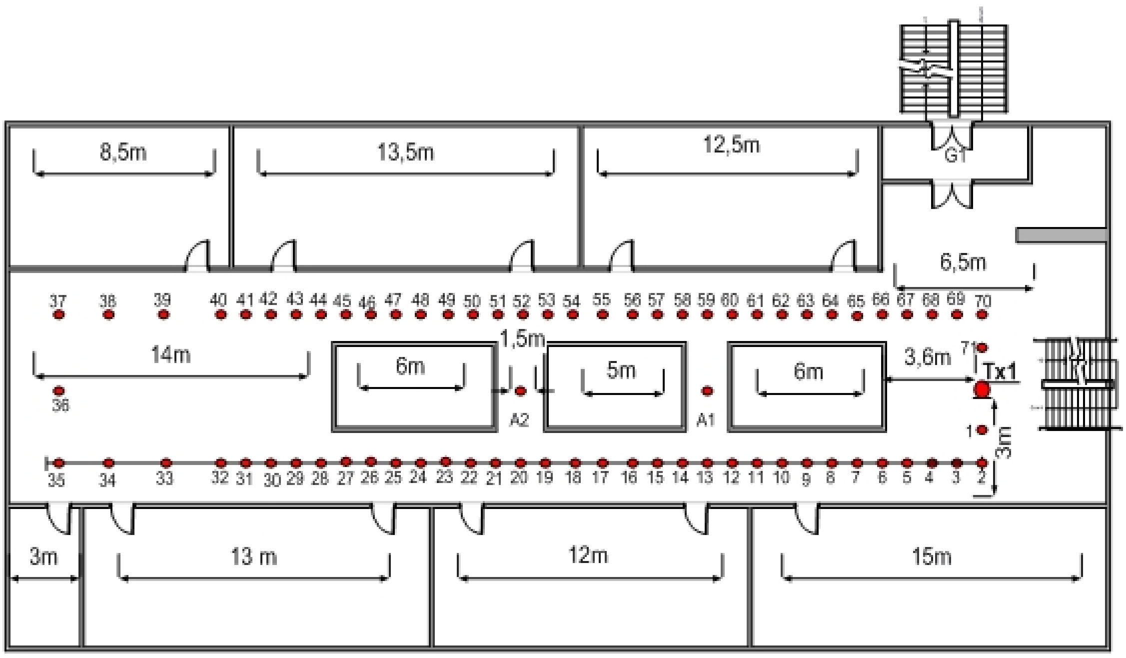

Fig 3.1. The layout of ground floor showing the transmitter position and the measurements points.

As known the received signal is composed of energy reflected, transmitted or diffracted by various parts of the buildings. The rays from the transmitter antenna reaches the receiver antenna after being reflected off walls, partitions, ceilings, floors, tables or being transmitted through walls and partitions. Consequently, the attenuation of the signal propagating in an indoor environment can be characterized by the geometrical and electrical properties of the construction materials. Therefore, to apply propagation models correctly and efficiently, it is necessary to obtain expressions defining these properties.

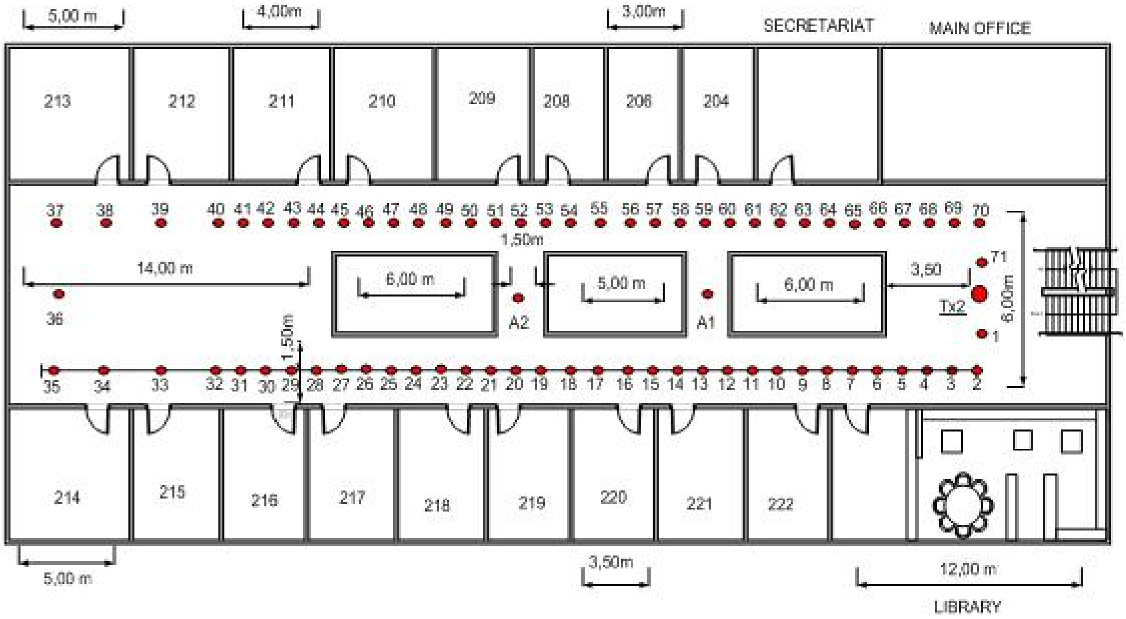

Figure 3.2.The plan of floor 1 showing the transmitter position and the the measurements points.

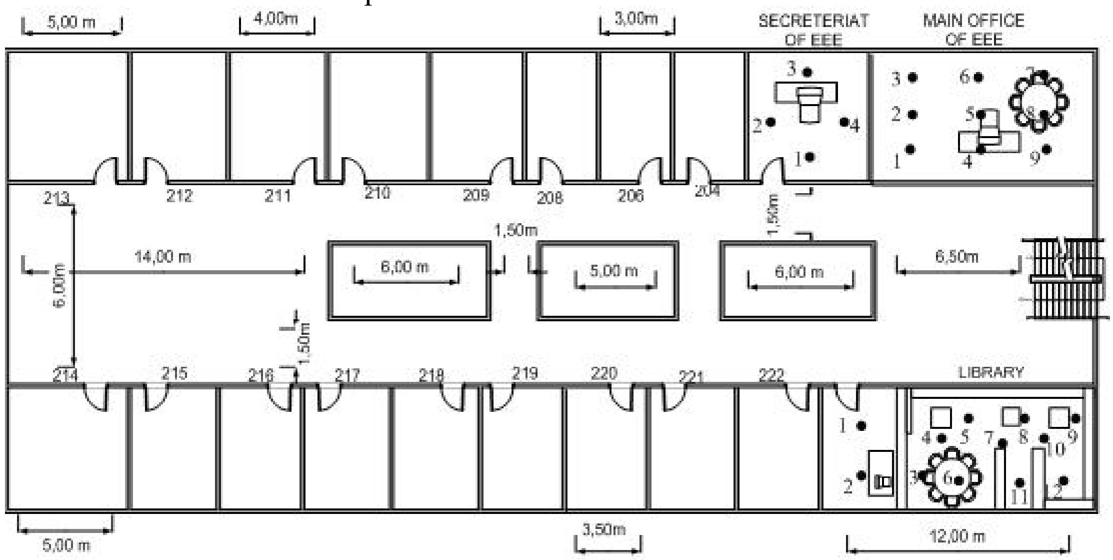

Figure 3.3. Measurement points at library, main Office and secretariat rooms in building.

4. EXPERIMETAL and THEORETICAL INVESTIGATION

In this section, the results are given for measurements and calculations accomplished by using empirical model and ray tracing method. In this study area, the variation in signal strength is investigated LOS and NLOS conditions. During indoor propagation, the first significant effect is an abrupt signal decay when a signal crosses a wall. The wall loss factor depend on frequency, wall thickness and the type of the material .

The measurements were made along the corridor using omni directional antennas. Also, the position of the transmitter is shown in the figure. Measurements were performed along the two sides of the corridor at symmetric points and rooms. The corridor tests consisted of taking measurements at 0.9 meter intervals along the length of the corridor. The room tests consisted of taking measurements at different points in the room, namely each corner and the centre of the room.

Here, a calculation using the empirical model is done to compare with the measurements results. For this calculation FAF and WAF was taken 20 dBm and 4 dBm for each obstruction, respectively. The actual signal strength is measured in dBm which is dB decibels referenced to one mW. Firstly, the transmitter Tx was located on ground floor and receiver which was positioned at a height of 1,5 m above ground, and moved along the corridor. By locating the transmitter at different places at a height 2 m above ground level, receiver signal level were obtained at different places (rooms, labs and corridors) of the building.

Since environment condition varies greatly due to people motion, measurements are performed during afternoon also, but no significant signal time variation is detected. The measurement value corresponding to a single point is the average of the 10 instantaneous successive received signal levels and each measurements were taken about between 4 to 6 minutes. This allows to minimize the possible remaining weak time fluctuations.

4.1. Comparison Of Measurements With Empirical Model Results

The measurements were performed at different points in the corridors, at different floors and different rooms in the building. The transmitter is Tems light Indoor type, and TEMS Investigation 3.02 & Ericson T28s measurement set and a Laptop were used. Tems Light Indoor transmitter output power is 17 dBm and attenuator is 12 dBm. The antenna model is Kathrein K 737 031 with a gain of 2 dBm. Signal frequency is 900 MHz, at canal 124 (=920 MHz) and the length of the feeder is 0.5 meter with 0 dB loss. When measurements are taken, TEMS investigation equipment is locked with transmitter at same canal, thus the measurements aren't effected by the other propagation mechanisms. And Laptop saves the received signal power.

(a)

(b)

Figure 4.1. Measurement equipments, (a) transmitter antenna for indoor, (b) Laptop power and TEMS investigation.

4.1.1. Test Along Corridors

The corridor test was performed in order to evaluate how much effect the corridor would have on a signal transmitted from one end to the other. Data were taken at 73 different points (Figure 3.1) where propagation measurements were made with the Tx placed on ground floor and the results are shown in Table 4.1. Here, a comparison between measurements and calculation using the empirical indoor propagation model which contains unit loss, floor attenuation, wall attenuation and loss which depend on distance is given.

Table 4.1. Comparison points and results for ground.

Point	d (m)	Meas. (dBm)	Empirical model (dBm)	Point	d (m)	Meas. (dBm)	Empirical model (dBm)
1	1,5	-38	-38,13	38	31,08	-70	-64,46
2	2,25	-39	-41,65	39	29,09	-69	-63,88
3	2,42	-38	-42,3	40	27,09	-66	-63,27
4	2,88	-39	-43,8	41	26,2	-64	-62,97
5	3,51	-40	-45,53	42	25,3	-64	-62,67
6	4,25	-41	-47,17	43	24,4	-63	-62,36
7	5,03	-42	-48,64	44	23,51	-63	-62,03
8	5,85	-42	-49,95	45	22,61	-61	-61,7
9	6,69	-44	-51,12	46	21,72	-60	-61,35
10	7,54	-45	-52,16	47	20,82	-60	-60,98
11	8,41	-46	-53,1	48	19,93	-58	-60,6
12	9,28	-49	-53,96	49	19,03	-60	-60,2
13	10,15	-51	-54,74	50	18,14	-60	-59,78
14	11,03	-50	-55,46	51	17,25	-64	-59,34
15	11,91	-53	-56,13	52	16,36	-66	-58,88
16	12,8	-54	-56,75	53	15,46	-63	-58,4
17	13,69	-56	-57,34	54	14,57	-59	-57,88
18	14,57	-56	-57,88	55	13,69	-58	-57,34
19	15,46	-61	-58,4	56	12,8	-55	-56,75
20	16,36	-63	-58,88	57	11,91	-56	-56,13
21	17,25	-63	-59,34	58	11,03	-52	-55,46
22	18,14	-58	-59,78	59	10,15	-52	-54,74
23	19,03	-55	-60,2	60	9,28	-50	-53,96
24	19,93	-56	-60,6	61	8,41	-47	-53,1
25	20,82	-57	-60,98	62	7,54	-46	-52,16
26	21,72	-57	-61,35	63	6,69	-44	-51,12
27	22,61	-58	-61,7	64	5,85	-42	-49,95
28	23,51	-61	-62,03	65	5,03	-41	-48,64
29	24,4	-61	-62,36	66	4,25	-40	-47,17

30	25,3	-62	-62,67	67	3,51	-39	-45,53
31	26,2	-62	-62,97	68	2,88	-39	-43,8
32	27,09	-63	-63,27	69	2,42	-38	-42,3
33	29,09	-65	-63,88	70	2,25	-38	-41,65
34	31,08	-66	-64,46	71	1,5	-38	-38,13
35	33,08	-68	-65	A1	10,4	-64	-70,52
36	33	-75	-112,98	A2	16,8	-66	-91,71
37	33,08	-71	-65				

Table 4.1., shows the median power level over the band (850–950 MHz) for each measurement location, where the median was taken over the dBm power levels. Typically wave propagation within the same floor, the mean path loss in dB increases exponentially with distance. The number of walls between transmitter and receiver introduces extra losses to the received signal level. Results show that the model has some deficiencies and at the points At A1 and A2, the deficiencies become evident. Results at these points, empirical model is much more lossy but in fact there is not that much loss at the received signal level. Because, while wall attenuation increases reflected and diffracted ray contributions to the points A1 and A2 also increases. This is why the, received power signal is much more than calculated value. The effect of walls for points 1 to 8 and points 65 to 71 are not considered in the calculations, because, there is LOS propagation between the source point and the observation points. But for points 8 to 20 and from points 51 to 64, the wall effects are included and it cause additional loss at the signal power. For the other points, a fixed value is added to calculate the signal level. Transmitted ray effects have been added to calculation for point A2 and point 36 where the rays are transmitted four times and six times, respectively.

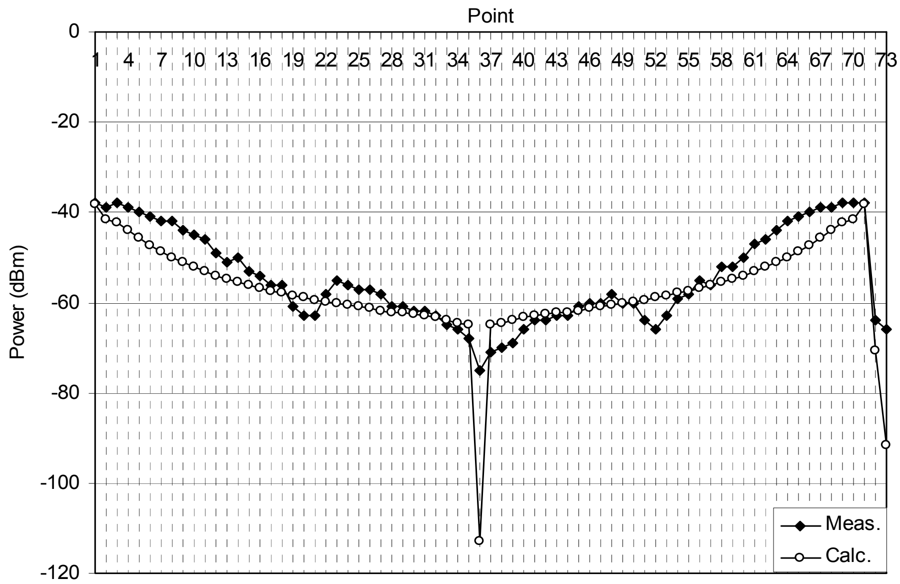

Figure 4.2. Graph of comparison between measurements and calculated for ground.

In Figure 3.2., Tx was placed on the 1st Floor and the results were taken along the corridors at 73 points where propagation measurements were made. The results are shown in Table 4.2., and the most lossy points are A1 and A2 as expected.

Table 4.2. Comparisons points and results for floor 1.

Point	d (m)	Meas. (dBm)	Empirical model (dBm)	Point	d (m)	Meas. (dBm)	Empirical model (dBm)
1	1,5	-38	-38,13	38	31,08	-68	-64,46
2	2,25	-39	-41,65	39	29,09	-67	-63,88
3	2,42	-38	-42,3	40	27,09	-66	-63,27
4	2,88	-39	-43,8	41	26,2	-65	-62,97
5	3,51	-39	-45,53	42	25,3	-65	-62,67
6	4,25	-39	-47,17	43	24,4	-64	-62,36
7	5,03	-40	-48,64	44	23,51	-63	-62,03
8	5,85	-41	-49,95	45	22,61	-63	-61,7
9	6,69	-42	-51,12	46	21,72	-62	-61,35
10	7,54	-42	-52,16	47	20,82	-62	-60,98

11	8,41	-44	-53,1	48	19,93	-60	-60,6
12	9,28	-47	-53,96	49	19,03	-61	-60,2
13	10,15	-51	-54,74	50	18,14	-59	-59,78
14	11,03	-50	-55,46	51	17,25	-59	-59,34
15	11,91	-51	-56,13	52	16,36	-61	-58,88
16	12,8	-51	-56,75	53	15,46	-56	-58,4
17	13,69	-52	-57,34	54	14,57	-56	-57,88
18	14,57	-54	-57,88	55	13,69	-54	-57,34
19	15,46	-55	-58,4	56	12,8	-53	-56,75
20	16,36	-59	-58,88	57	11,91	-52	-56,13
21	17,25	-58	-59,34	58	11,03	-53	-55,46
22	18,14	-58	-59,78	59	10,15	-54	-54,74
23	19,03	-59	-60,2	60	9,28	-49	-53,96
24	19,93	-57	-60,6	61	8,41	-46	-53,1
25	20,82	-59	-60,98	62	7,54	-45	-52,16
26	21,72	-57	-61,35	63	6,69	-43	-51,12
27	22,61	-57	-61,7	64	5,85	-41	-49,95
28	23,51	-58	-62,03	65	5,03	-41	-48,64
29	24,4	-60	-62,36	66	4,25	-39	-47,17
30	25,3	-60	-62,67	67	3,51	-39	-45,53
31	26,2	-62	-62,97	68	2,88	-38	-43,8
32	27,09	-62	-63,27	69	2,42	-38	-42,3
33	29,09	-64	-63,88	70	2,25	-38	-41,65
34	31,08	-65	-64,46	71	1,5	-38	-38,13
35	33,08	-67	-65	A1	10,4	-65	-70,52
36	33	-72	-112,98	A2	16,8	-68	-91,71
37	33,08	-69	-65				

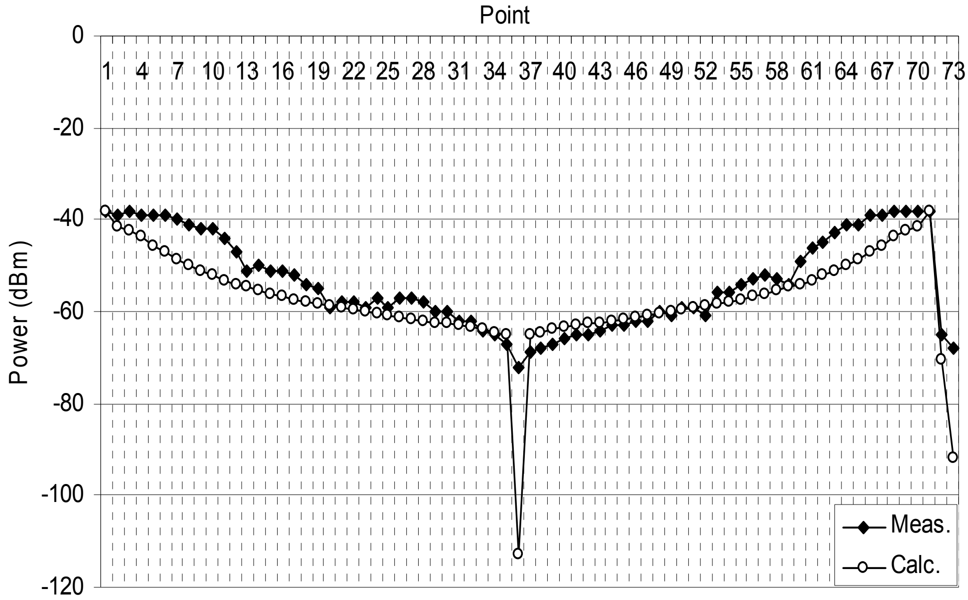

Figure 4.3. Plot of comparison between measurements and calculated of power for floor 1.

As seen in Figure 4.3., the results show that the level of the signal power decreases by distance. But the corridors behave as wave guides. Especially end of the corridor illumination is satisfied that reflected rays and the diffracted rays has a significant effect particularly evident in the NLOS zone.

4.1.2. Propagation Between Floors

For this case, the measurements were taken at the 1st Floor when Tx is located at ground Floor which requires both WAF and FAF to be taken into consideration. The floor attenuation factor is between 15 and 30 dBm at 900 MHz and increases by distance between the receiver and the transmitter.

Table 4.3. Comparison between measurements and calculated for Tx at ground, Rx at floor1 .

Point	d (m)	Meas. (dBm)	Empirical model (dBm)	Point	d (m)	Meas. (dBm)	Empirical model (dBm)
1	1,5	-58	-58,13	37	33,08	-108	-85

2	2,25	-59	-61,65	38	31,08	-106	-84,46
3	2,42	-61	-62,3	39	29,09	-106	-83,88
4	2,88	-61	-63,8	40	27,09	-100	-83,27
5	3,51	-63	-65,53	41	26,2	-101	-82,97
6	4,25	-64	-67,17	42	25,3	-98	-82,67
7	5,03	-64	-68,64	43	24,4	-98	-82,36
8	5,85	-66	-69,95	44	23,51	-96	-82,03
9	6,69	-67	-71,12	45	22,61	-97	-81,7
10	7,54	-70	-72,16	46	21,72	-94	-81,35
11	8,41	-70	-73,1	47	20,82	-93	-80,98
12	9,28	-73	-73,96	48	19,93	-91	-80,6
13	10,15	-74	-74,74	49	19,03	-92	-80,2
14	11,03	-74	-75,46	50	18,14	-90	-79,78
15	11,91	-75	-76,13	51	17,25	-87	-79,34
16	12,8	-78	-76,75	52	16,36	-85	-78,88
17	13,69	-78	-77,34	53	15,46	-84	-78,4
18	14,57	-79	-77,88	54	14,57	-81	-77,88
19	15,46	-81	-78,4	55	13,69	-81	-77,34
20	16,36	-81	-78,88	56	12,8	-79	-76,75
21	17,25	-83	-79,34	57	11,91	-80	-76,13
22	18,14	-83	-79,78	58	11,03	-77	-75,46
23	19,03	-85	-80,2	59	10,15	-76	-74,74
24	19,93	-86	-80,6	60	9,28	-75	-73,96
25	20,82	-89	-80,98	61	8,41	-75	-73,1
26	21,72	-89	-81,35	62	7,54	-72	-72,16
27	22,61	-92	-81,7	63	6,69	-70	-71,12
28	23,51	-96	-82,03	64	5,85	-70	-69,95
29	24,4	-96	-82,36	65	5,03	-68	-68,64
30	25,3	-98	-82,67	66	4,25	-67	-67,17
31	26,2	-97	-82,97	67	3,51	-64	-65,53
32	27,09	-98	-83,27	68	2,88	-63	-63,8
33	29,09	-101	-83,88	69	2,42	-61	-62,3
34	31,08	-104	-84,46	70	2,25	-60	-61,65
35	33,08	-105	-85	71	1,5	-57	-58,13
36	33	-110	-84,98				

Figure 4.4. shows that the measured and calculated results are in good agreement at points where Tx is not close to the observation but when go far away from Tx, difference of results are higher.

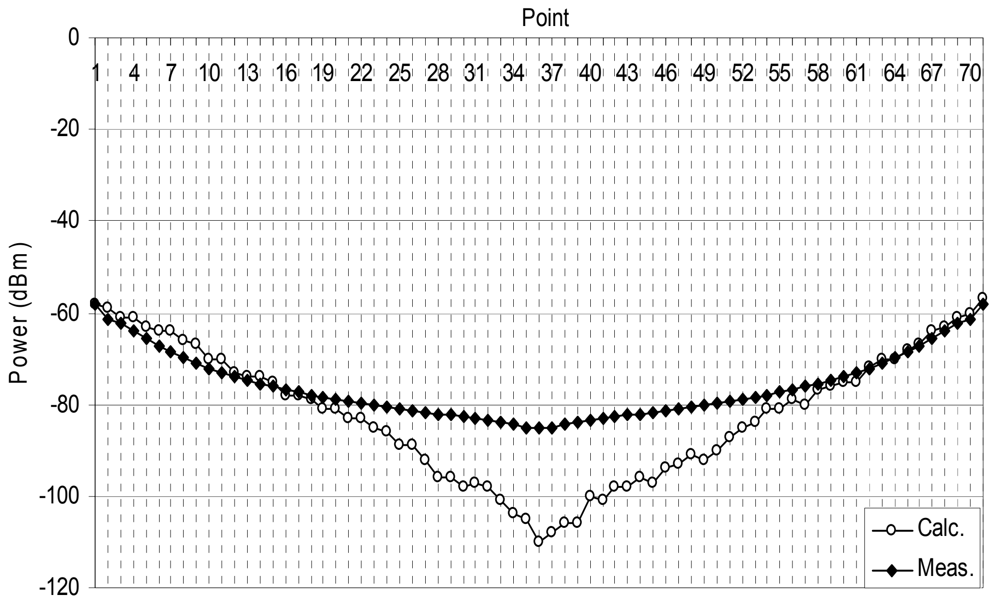

Figure 4.4. Plot of comparison between measurements and calculated of power, Tx at ground and measurements at floor1.

4.1.3. Measurements in Rooms

This is a library with a layout shown in Figure 3.3. The room contains several doors, desk , shelves, one personal computers and standard library equipment,. Walls are made of concrete blocks (rough surface). The room tests consisted of taking measurements at different points in the room, namely each corner and the centre of the room. In this room, there are a lot of signals which reflected and diffracted. The rays reaches into room passing through from wall, and then reaches received points. First, power of signal decrease depend on wall and then rays advance into room. And this cause attenuation at signal level which about 15-30 dBm. Of course this is depend on distance between receiver and transmitter and furniture which are in door. They influence received power of signal.

Here there are comparisons for other rooms between calculated and measurements. Of course, furniture effects, equipment effects and etc. isn't joined for calculated.

Table 4.4. Comparisons for EEE library.

Point	d (m)	Measurement (dBm)	Empirical model (dBm)
1	7,3	-55	-49,27
2	9,2	-57	-51,28
3	8	-58	-50,06
4	5,9	-58	-47,42
5	4,4	-61	-44,87
6	7,5	-60	-49,50
7	5,8	-61	-47,27
8	5,2	-63	-46,32
9	6,4	-65	-48,12
10	6,8	-63	-48,65
11	7,7	-67	-49,73
12	8,5	-69	-50,59

According to measurements, results are more loss than calculated. Actually it is good agreement, because in real in this room there are many reflected and diffracted rays from office furniture and so signal level is more loss than calculated which doesn't contain effects of reflected and diffracted rays. And in same way at main office, calculated is more loss than measurements. Because signal which just one wall passing and there is no more loss of signal level. And it shows that this empirical model has some deficiencies to explain indoor propagation.

Table 4.5. Comparison for Electrical Engineering main office.

Point	d (m)	Measurement (dBm)	Empirical model (dBm)
1	5,2	-47	-46,32
2	6,4	-51	-48,12

3	8	-54	-50,06
4	4,4	-46	-44,87
5	6,2	-50	-47,85
6	7,7	-54	-49,73
7	8,2	-56	-50,28
8	6,9	-55	-48,78
9	5,4	-52	-46,65

This is the department of Electrical-Electronic Engineering secretariat. The room contains two desk with standard secretarial accessories. There is personal computers, a printer, fax machine. Most of the area is empty. Walls have rough surface. The state of the door (open or closed) affects the power levels, and this indicates that most of the radiation penetrates directly through the wall.

Table 4.6. Comparison for Electrical-Electronic Engineering secretariat.

Point	d (m)	Measurement (dBm) (door is close)	Measurement (dBm) (door is open)	Empirical model (dBm)
1	7,5	-54	-50	-60,11
2	9,7	-50	-49	-62,34
3	9,9	-55	-51	-62,52
4	7,8	-53	-50	-60,45

The results of measurements show that when door is open, there is a changing about signal level. It is actually not very interesting result. It is expected. When door is open, received signal level will increase than door is closed. Because when signal passing through of door it cause loss of received signal level.

4.2. Comparisons Between Measurements, Empirical Model And Ray Tracing Technique Results

It is known that radio propagation in a building is much more complex than propagation in free space. At indoor radio communications systems the interaction of signals with various materials cause attenuation and the signal strength on open plan offices, walls, floors, type of construction materials, density of personnel, furniture, etc.

In this part, ray tracing technique will be applied to calculate the signal strengths. The empirical model assumes that the contribution of the reflected and diffracted rays are negligible. It is obvious that this not true in all cases and sometimes this approach may not be able to explain the propagation mechanism correctly. But theoretically ray-tracing technique is capable of considering all possible rays for indoor propagation phenomena. As the order of scattering mechanism is increased, the complexity of calculating the components of the scattered field also increases.

Therefore, in this work three groups of rays are considered. The first group is the Reflected-Reflected (RR) and Reflected-Reflected-Reflected (RRR) group, which consists of rays reflected along both main (or LOS) corridor and perpendicular (or NLOS) corridor. The second group of rays is the Reflected-Diffracted-Reflected (RDR) or Diffracted-Reflected-Reflected group, which consists of rays that may be reflected along the LOS corridor, then diffracted at the corner, and that may be reflected again along the NLOS corridor. And the last group consist of various type of transmitted rays. Higher order scattered terms are assumed to be negligible and they are not taken into consideration.

The field strength at the receiver is obtained as the sum of the fields associated with the rays that connect the transmitting antenna to the receiver. The wall attenuation factor (WAF) is calculated as the sum of the reflected and diffracted rays, and the floor attenuation factor (FAF) is the sum of the rays transmitted through the floor. The measured signal levels at NLOS locations are higher than the values predicted by the path loss prediction formula. This difference is partly due to the presence of indirect rays or diffracted rays. As is stated in Section 2, the corner diffracted field can be written as follows by GTD,

$$E^d = E^i(w).D.A(w,j).\sqrt{\frac{s_{iw}}{s_{wj}.s_{ij}}}e^{-jks_{wj}}$$

with the diffraction coefficient for a wedge is given as

$$D_h = \frac{e^{i\frac{\pi}{4}}.\sin\frac{\pi}{n}}{n.\sqrt{2\pi k}.\sin\beta_0}\left[(\cos\frac{\pi}{n}-\cos\frac{\psi-\psi_o}{n})^{-1}+(\cos\frac{\pi}{n}-\cos\frac{\psi+\psi_o}{n})^{-1}\right]$$

Here, the angels ψ and ψ_0 define the direction of propagation of the incident and reflected fields. β_0 is the angle between incident ray and the edge of the wedge. The wave number k=(2πf/c) and is equal to 6π at 900 MHz. The internal angle of the wedge is equal to $\alpha = (2-n)\pi$ and so n has the value of $n = (2-\alpha/\pi)$ and it is equal to 3/2 for the present case. The diffraction coefficient D is calculated to be 0.262exp(-jπ/4).

The application of this technique requires to know the value of dielectric constants on the operation frequency, so that the reflection, transmission and diffraction coefficients can be determined. At 900 MHz, the complex dielectric constant of the wall is taken as $\varepsilon_r = 5.1 - j0.20$ for brick-wall and as ε_r = 10-j2.0 for floor and also the reflection and transmission coefficients are 0.382 and 0.212, respectively (Yang C.,1998).

To verify the accuracy of the ray tracing technique, propagation measurements taken the First floor are compared with the calculated values at points (7,12,16,18 and A1) on First and Second floors. The floor attenuation is considered when Tx is at ground floor and Rx on First and Second floors.

The results obtained by theoretical predictions, i.e. the empirical method and the ray tracing technique, are compared with the measurements.

Table 4.7. Comparisons between the empirical and the ray tracing model for for some points on Floor1.

Point	Measured	Empirical Model (dBm)	Ray Tracing Model (dBm)
7	-40,00	-48	-41,61
12	-47,00	-53,96	-49,91
16	-54,00	-56,75	-52,383
18	-54,00	-57,88	-55,68
A1	-65,00	-70,95	-64,03

Table 4.8. Comparisons between the empirical and the ray tracing model for main office of EEE.

Point	Measurement (dBm)	Empirical Model (dBm)	Ray Tracing Model (dBm)
4	-47	-44,87	-47,8
6	-54	-49,73	-57
7	-56	-50,28	-58
9	-52	-46,65	-51

Table 4.9. Comparisons between the empirical and the ray tracing model for library of EEE.

Point	Measurement (dBm)	Empirical Model (dBm)	Ray Tracing Model (dBm)
5	-61	-44,87	-59
9	-65	-48,12	-62,6
11	-67	-49,73	-65,73
12	-69	-50,59	-67,6

In Tables 4.8. and 4. 9. indicate a comparison for empirical and ray tracing model. Results show that ray tracing model provide more true conclusions. For results of main office, the empirical and ray tracing model’s results are close, of course it is expected because there is a just one wall and signal encounter this wall and then arrive to receiver points. But for library, there are a wall and shelves which signal pass these obstacle and then arrive receiver point. Of course this shelf cause more loss at the signal level. And this effect isn’t contributed in the empirical model but in ray tracing technique, the effects is added into the calculation. Also, to measure the multiple floor attenuation and wall attenuation, the transmitter and receiver stations were located on different floors. Tx was placed on ground floor, the measurements were taken at same point but at different floor.

Table 4.10. Measurements points and results for tx at ground floor.

	Measurements (dBm)	Empirical Model (dBm)	Ray Tracing Model (dBm)
At same point on floor 1 ,whenTx is at ground floor	-57	-55,4	-56,33
At same point on floor 2, whenTx is at ground floor	-71	-83	-75

According to results of the measurements, the floor attenuation is -19dBm when Tx at ground Rx at floor 1.This is found that by the ray tracing technique as -18.33. And when Tx at ground Rx at floor 2, for measurements, floor attenuation is -33 dBm . This is found that by the ray tracing technique as -38 dBm. Consequently, results of ray tracing techniques are more correct than the results of the empirical model results. The number of walls between transmitter and receiver introduces extra losses to the received signal level.

5. CONCLUSION

This thesis has presented the results for an investigation of indoor radio wave propagation at 900 MHz in the Department of the Electrical Electronics Engineering building at the University of Çukurova. Propagation path loss is measured and compared with an empirical model and the ray tracing model.

The results show that good results are generally obtained by the empirical model. But during the situation of indoor radio propagation, structure of environment is the most effect on the propagation phenomena. The empirical model doesn't consider this effect in the calculation. The variation of building size, shape, structure, layout of rooms and, the type of construction materials, electromagnetic wave propagation inside a building is a complex and effect of these is important for indoor propagation. Measurements show that the propagation is strongly dependent on the rooms configurations and door is open or closed. The investigation of the indoor radio propagation processes shows that the electromagnetic field distribution is significantly influenced by the diffraction and reflection phenomena due to the presence of the structure of environment.

The signal behavior is effected by the propagation mechanisms. The most significant thing for indoor propagation all the effects can be considered in calculation with the model to do true approximate. For this, the ray tracing technique is used to explain and calculate for the effects of the propagation mechanisms in indoor environments. Results show that the ray tracing technique is more useful and consistent than the empirical model to explain propagation mechanism. But it is more complex and has high computations.

And additional, to know dielectric parameters of materials is more important for indoor radio propagation. For GSM frequencies, dielectric parameters of some materials are present. In this study dielectric properties (reflection, transmission coefficients and permittivity) are found for the concrete specimens between 8.4 GHz and 12 GHz. The various of dielectric properties are given for different thickness and different ratio of w/c. The electric constants vary quite smoothly and closely for different polarizations. And than, this measurements have been tried to formulate using by version of Matlab 7.0. These formulas could be used to find amplitude of reflection, transmission and diffraction coefficient for cement based materials which have same construction of materials, between 8.4 and 12 GHz. These formulas which are depend on frequency and thickness, give good agreements with measurements. Of course, this is a good approximate using by these formulations to find reflection, transmission coefficients and permittivity and use into the ray tracing technique.

Also, these information can be used to create a date base. And so, the program could be done to predict about indoor radio propagation by that date base.

REFERENCES

BERNARDİ, P., CİCHETTİ, R., and TESTA, O., June, 2004. An Accurate UTD Model for the Analysis of Complex Indoor Radio Environments in Microwave WLAN Systems. IEEE Transactions on Antennas and Propagation, Vol. 52, No. 6, 1509-1520.

BUTTERWORTH, K., SOWERBY, K.W., and WİLLİAMSON,A.G., September, 1996. A 1.8 GHz Indoor Wideband Propagation Study at The University of Auckland, 21p.

CHİN, C., and WANG, C., Oct. 5, 1998. Impact of Shapes of Buildings and Metallic Furniture on Indoor Multipath Environment and Bit-Error Rate Performance of Millimeter-Wave Channels, Microwave Opt. Technol. Lett., Vol. 19, No.2, pp. 137–142.

CLARKE, A., September 16, 2002a. A Reaction Diffusion Model for Wireless Indoor Propagation. Computer Engineering, University of Dublin.

______, February, 2002b. A Three Dimensional UTD Heuristic Diffraction Coefficient for Complex Penetrable Wedges, IEEE Trans. Antennas Propagat., Vol. 50, pp. 217–224.

DOBLE, J., 1996. Introduction to Radio Propagation For Fixed and Mobile Communications. Artech House, Boston-London, 189p.

GHODGAONKAR, D. K, VARADAN, V. V., and VARADAN, V. K., 1989. A Free-Space Method for Measurement of Dielectric Constants and Loss Tangents at Microwave Frequencies. IEEE Trans. on Instrum. and Meas., 37(3): 789-793.

KHARKOVSKY, S. N., ATİŞ, C. D., AKAY, M. F., and HASAR, U. C., 2001. Measurement and Monitoring of Microwave Reflection Properties of Cement-Based Materials for Propagation Modeling. 4th European Personal Mobile Communications Conference, Vienna, Austria.

MA, Z., and OKAMURA, S., 1999. Permittivity Determination Using Amplitudes of Transmission and Reflection Coefficients at Microwave Frequencies. IEEE Trans. on Microwave Theory and Tech., 47(5): 546-550.

RAPPAPORT, THEODORE, S., 1996. Wireless Communications: Principles and Practice, Prentice Hall Publications, NJ.

TAM, W. K., and TRAN, V. N., October, 1995. Propagation Modelling for Indoor Wireless Communication. Electronics & Communication Engineering Journal, pp. 221-228.

TORRES, R. P., VALLE, L., DOMINGO, M., LOREDO, S., and DİEZ, M. C., August 1999. An Engineering Tool for Planning and Design of Wireless Systems in Enclosed Spaces, IEEE Antennas Propagation Mag., Vol. 41, pp. 11–22.

VİNKO, E., RUSTAKO A.J., JR. and ROMAN, R.S., .AT&T Bell Laboratories Holmdel, NJ 07733. Diffraction Around Corners And Its Effects On The Mıcrocell Coverage Area In Urban And Suburban Envıronments At 900 Mhz, 2 GHz, And 6 GHz, 1998.

YANG C., Member IEEE, Wu B-C., and Ko C.-J., A Ray-Tracing Method for Modeling Indoor Wave Propagation and Penetration, IEEE Transactıons On Antennas And Propagatıon, Vol. 46, No. 6, June 1998.

BIOGRAPHY

I was born in Adana, Turkey, on October 20, 1979. I graduated from Faculty of Engineering and Architecture of Niğde University in 2001, Niğde, Turkey. My current areas of research involve microwave, indoor propagation, measuring the electrical properties of materials and telecommunications (GSM).

APPENDIX – Derivation Of Dielectric Properties Of Materials

When a signal is transmitted through or reflected off a wall or a partition, the degree of signal attenuation and the amount of phase change depend on the complex transmission and reflection coefficients, respectively. At indoor propagation knowing construction of materials which signal encounter, is so important to predict signal behaviors. Since those properties depend not only on the constitutive parameters of the buildings but also on the thicknesses of the structures. Here a free space approach is used to measure the dielectric constants of the walls. So, the amplitude of reflection and transmission coefficients and permittivity for concrete construction at X band (8.4 GHZ – 12 GHz) and at different polarizations are measured and these results are used for formulation at different thicknesses and between 8.4 GHz and 12 GHZ frequencies.

1-)Transmission And Reflection of A Radio Signal

The transmission coefficient is defined as the ratio of the transmitted to the incident electric-field strengths and the reflection coefficient is defined as the ratio of the reflected to the incident electric-field strengths.

Here, the concretes which have different thicknesses and different ratio of water/cement were measured between 8.4 GHz and 12 GHz and at different polarizations, vertical and horizontal. The concrete specimens which come into existence cement, sand, water and air were used. The cement used in the experiment is the ASTM Type 1 normal Portland cement (NPC). Well-graded, uncrushed-clean, quartzite, natural sand is used. Mortar specimens are prepared with different w/c ratios using the mix proportions of 1:1.5 cement and sand by weight respectively. Figure A.1 shows the incident, reflected and transmitted field components that occur due to the presence of a dielectric slab in free space. Region I and III are free space and region II is the “sample” with relative dielectric permittivity $\varepsilon_r \neq 1$ and $\mu_r = 1$.

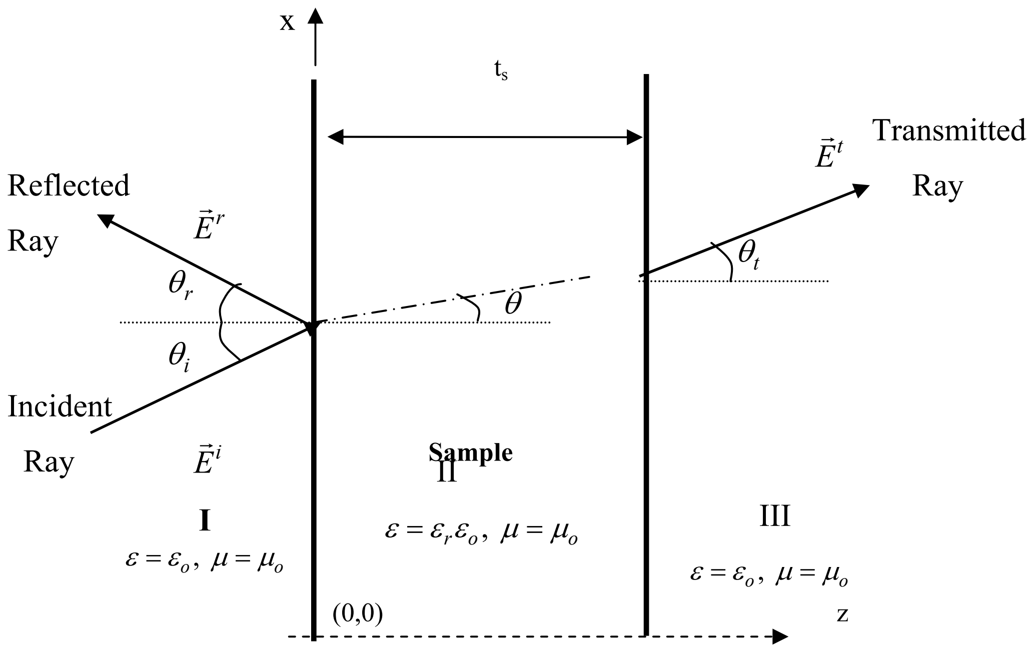

Figure A.1. Figure of incident field, reflected field and transmitted field from sample and to measure of permittivity of a material using the free-space method.

The wave passes from the radiating antenna to the receiving antenna through the air and sample. Reflection occurs at the interface of the air-sample and multiple reflections occur between the two sides of the sample.

Using the ray-tracing method, the total reflection coefficient can be written as (Kharkovsky, Atiş and Hasar, 2001).

$$r = r_{12} + t_{12} r_{23} t_{21} e^{-j2\Theta} + t_{12} r_{21} r_{23}^2 t_{21} e^{-j4\Theta} \ldots \tag{1}$$

Where, the reflection coefficients are denoted by r_{12} at I, r_{21} at II, r_{23} at III and the transmission coefficients are denoted by t_{12} at I, t_{21} at II and t_{23} at III, respectively. Here

$$\Theta = k_s t_s \cos\theta, \qquad k_s = 2\pi / \lambda_0 \sqrt{\varepsilon_r}, \\ \varepsilon = \varepsilon_o \varepsilon_r, \qquad \varepsilon_r = \varepsilon_r' - j\varepsilon_r'', \qquad \cos\theta = \sqrt{1 - 1/\varepsilon_r \sin^2\theta_i}. \tag{2}$$

In equations $\lambda_o, t_s, \varepsilon$, and θ_i are the wavelength in free-space, thickness of the regions, dielectric permittivity of the material, and incident angle between normal of the boundary and incident wave, respectively. Equation (1) can be written in a more suitable form as,

$$r = r_{12} + r_{23}t_{12}t_{21}e^{-j2\Theta}\left[1 + r_{21}r_{23}e^{-j2\Theta} + ...\right]. \quad (3)$$

The expression in square brackets is in geometric series and when simplified,

$$r = r_{12} + \frac{r_{23}t_{12}t_{21}e^{-j2\Theta}}{1 - r_{21}r_{23}e^{-j2\Theta}} \quad (4)$$

is obtained. Regarding the following well-known relations,

$$\begin{aligned} &r_{21} = -r_{12}, \quad r_{23} = -r_{12} \\ &t_{12} = 1 + r_{12} \\ &t_{21} = 1 + r_{21} = 1 - r_{12} \end{aligned} \quad (5)$$

(4) becomes

$$r = \frac{r_{12}(1 - e^{-j2\Theta})}{1 - r_{12}^2 e^{-j2\Theta}}. \quad (6)$$

And by using a similar procedure, the transmission coefficient, *t*, can be expressed as

$$t = \frac{(1 - r_{12}^2)e^{-j\Theta}}{1 - r_{12}^2 e^{-j2\Theta}}. \quad (7)$$

The sample is assumed to be lossy enough so that the multiple reflections between the two surfaces of the sample can be neglected by selecting a thickness that ensures at least 10 dB attenuation, (Trabelsi et. al. 1998). According to this assumption, only the first terms of the geometric series are sufficient to represent the reflection and transmission coefficients:

$$\begin{aligned} &r = r_{12} \\ &t = (1 - r_{12}^2)e^{-j\Theta}. \end{aligned} \quad (8)$$

The complex transmission and reflection coefficients for horizontal polarization are,

$$t_h = \frac{E_t}{E_i} = \frac{2\cos\theta_i}{\cos\theta_i + (\frac{\varepsilon}{\varepsilon_0} - \sin^2\theta_i)^{1/2}} \quad \text{and} \quad r_h = \frac{E_r}{E_i} = \frac{\cos\theta_i - (\frac{\varepsilon}{\varepsilon_0} - \sin^2\theta_i)^{1/2}}{\cos\theta_i + (\frac{\varepsilon}{\varepsilon_0} - \sin^2\theta_i)^{1/2}} \quad (9)$$

The complex transmission and reflection coefficients for vertical polarization are,

$$t_v = \frac{E_t}{E_i} = \frac{2\cos\theta_i}{(\frac{\varepsilon}{\varepsilon_0})^{1/2}\cos\theta_i + (1 - \frac{\varepsilon}{\varepsilon_0}\sin^2\theta_i)^{1/2}} \quad \text{and} \qquad (10)$$

$$r_v = \frac{E_r}{E_i} = \frac{\frac{\varepsilon}{\varepsilon_0}\cos\theta_i - (\frac{\varepsilon}{\varepsilon_0} - \sin^2\theta_i)^{1/2}}{\frac{\varepsilon}{\varepsilon_0}\cos\theta_i + (\frac{\varepsilon}{\varepsilon_0} - \sin^2\theta_i)^{1/2}} \quad . \qquad (11)$$

2-)Measurement Setup

In the well known free space method the material to be measured is placed on the propagation path of the microwave signal. The sample illuminated by a transmitting antenna and the signal propagates through the material under test, and then it is received by receiving antenna and detected. The schematic diagram of the measurement set up used for the determination of the permittivity of the lossy materials using only amplitudes of reflection and transmission coefficients is shown Fig. A.2..

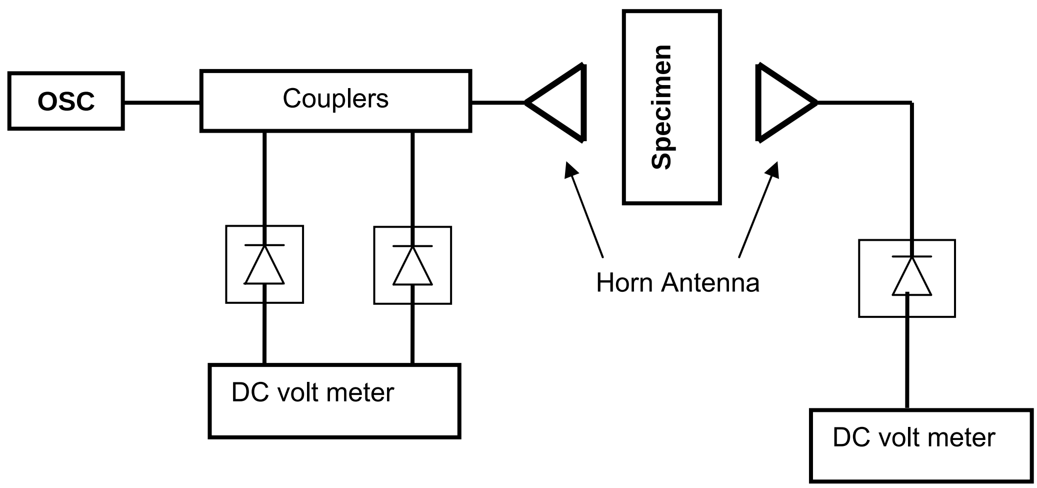

Figure A.2. Schematic diagram of the measurement set up.

Here a microwave oscillator (OSC), two directional couplers, square law detector, attenuator, two DC voltmeters and two horn antennas (HP 2163983) are used. It is consists of a OSC, feeds the system, modulated by a 1 kHz signal, square-law detector and VSWR meter are used as an attenuation meter (T meter) to measure the amplitude of the transmission coefficient in dB. A simple reflectometer built from discrete components (two directional couplers, a detector and DC voltmeter) is used to determine the amplitude of the reflection coefficient. Output power of the oscillator is not greater than 10 mW at frequencies of X-band (8-12 GHz). The samples is placed in free space between the two horn antennas. The two antennas, transmitting and receiving antenna have the same specifications. The output of the square-law detector is approximately directly proportional to $|r|^2$. The reference level of these measurements is determined for the case when there is no sample between the horn antennas.

3-) Results for Different Specimens

Twelve samples were used for the measurements, with different thicknesses and different water/cement ratio. The measurements were taken at different polarizations, and between 8.4 GHz and 12 GHz. The water-cement ratio and the dimensions of the are as follows:

Sample 1; dimensions : 9.8 x15 x15 cm, ratio of water to cement: 0.4

Sample 2; dimensions : 9.8 x15 x15 cm, ratio of water to cement :0.5

Sample 3; dimensions : 9.8 x15 x15 cm, ratio of water to cement: 0.55

Sample 4; dimensions : 9,8 x15 x15 cm, ratio of water to cement: 0.6

Sample 5; dimensions : 9,8 x15 x15 cm, ratio of water to cement: 0.75

Sample 6; dimensions : 7.5 x15 x15 cm, ratio of water to cement: 0.4

Sample 7; dimensions : 5 x15 x15 cm, ratio of water to cement : 0.4

Sample 8; dimensions : 3 x15 x 15 cm, ratio of water to cement : 0.4

Sample 9; dimensions : 3 x15 x15 cm, ratio of water to cement w/c:0.5

Sample 10; dimensions : 3 x15 x 15 cm, ratio of water to cement : 0.6

Sample 11; dimensions : 3 x15 x15 cm, ratio of water to cement : 0.65

Sample 12; dimensions :15x 15 x 15 cm, ratio of water to cement: 0.4

For all samples the measurements between 8.4 GHz and 12 GHz at vertical and horizontal polarizations are given below.

TableA.1. Permittivity, reflection and transmission coefficients for sample 1, at horizontal polarization.

F (GHZ)	Amplitude of Ref. Coef.	Amplitude of Trans. Coef.	Amplitude of Ref. Coef.(dB)	Amplitude of Trans. Coef.(dB)	Permittivity (ε_r)
8,4	0,3795	0,2739	8,42	11,25	4,9420
8,6	0,4000	0,2780	7,96	11,12	5,4444
8,8	0,3873	0,2850	8,24	10,90	5,1267
9	0,3873	0,2850	8,24	10,90	5,1267
9,2	0,4000	0,2622	7,96	11,63	5,4444
9,4	0,4243	0,2850	7,45	10,90	6,1198
9,6	0,4320	0,2582	7,29	11,76	6,3576
9,8	0,4339	0,2712	7,25	11,34	6,4146
10	0,4243	0,2437	7,45	12,26	6,1198
10,2	0,4000	0,2141	7,96	13,39	5,4444
10,4	0,3974	0,2115	8,02	13,49	5,3765
10,6	0,3843	0,1829	8,31	14,75	5,0552
10,8	0,3912	0,1681	8,15	15,49	5,2221
11	0,4000	0,1658	7,96	15,61	5,4444
11,2	0,4099	0,1500	7,75	16,48	5,7079
11,4	0,4227	0,1414	7,48	16,99	6,0730
11,6	0,4297	0,1494	7,34	16,52	6,2837
11,8	0,4382	0,1612	7,17	15,85	6,5528
12	0,4336	0,1500	7,26	16,48	6,4060

Table A.2. Permittivity, reflection and transmission coefficients for sample 1, at vertical polarization.

F (GHZ)	Amplitude of Ref. Coef.	Amplitude of Trans. Coef.	Amplitude of Ref. Coef.(dB)	Amplitude of Trans. Coef.(dB)	Permittivity (ε_r)
8,4	0,3651	0,2814	8,75	11,01	4,6240
8,6	0,3908	0,2812	8,16	11,02	5,2121
8,8	0,3821	0,2915	8,36	10,71	5,0031

9	0,3818	0,2887	8,36	10,79	4,9963
9,2	0,3933	0,2677	8,11	11,45	5,2734
9,4	0,4195	0,2903	7,54	10,74	5,9802
9,6	0,4243	0,2669	7,45	11,47	6,1198
9,8	0,4320	0,2708	7,29	11,35	6,3576
10	0,4183	0,2500	7,57	12,04	5,9457
10,2	0,3983	0,2206	8,00	13,13	5,4013
10,4	0,3924	0,2179	8,12	13,23	5,2523
10,6	0,3801	0,1852	8,40	14,65	4,9560
10,8	0,3864	0,1693	8,26	15,43	5,1060
11	0,3957	0,1690	8,05	15,44	5,3341
11,2	0,4044	0,1546	7,86	16,22	5,5605
11,4	0,4171	0,1458	7,59	16,73	5,9113
11,6	0,4243	0,1500	7,45	16,48	6,1198
11,8	0,4320	0,1633	7,29	15,74	6,3576
12	0,4308	0,1523	7,31	16,35	6,3191

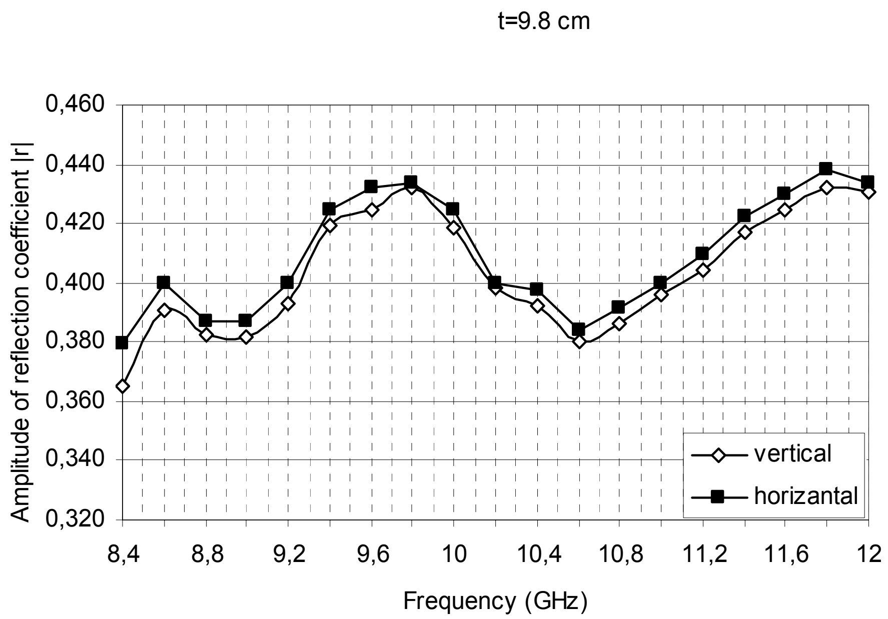

Figure A.3. Plot of reflection coefficients for sample 1, at horizontal and vertical polarizations.

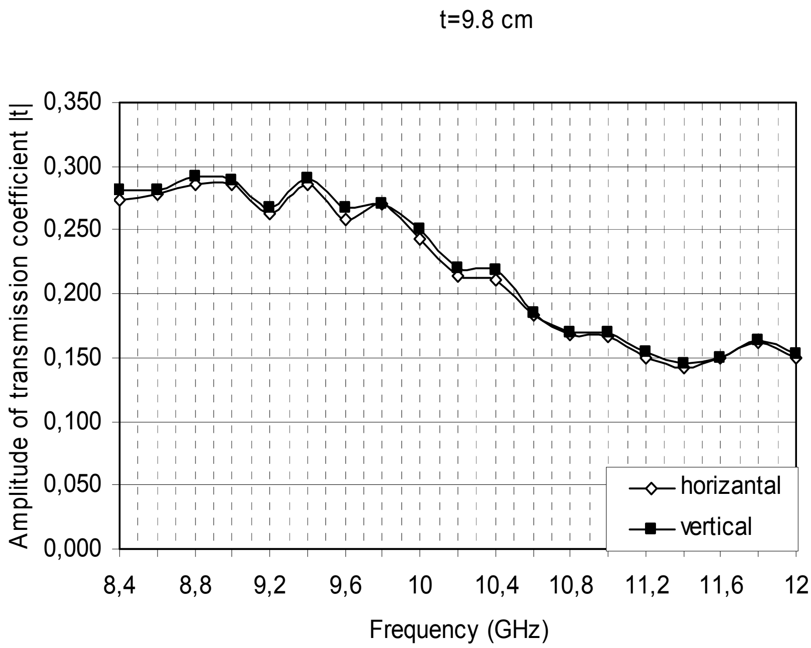

Figure A.4. Plot of transmission coefficients for sample 1, at horizontal and vertical polarizations.

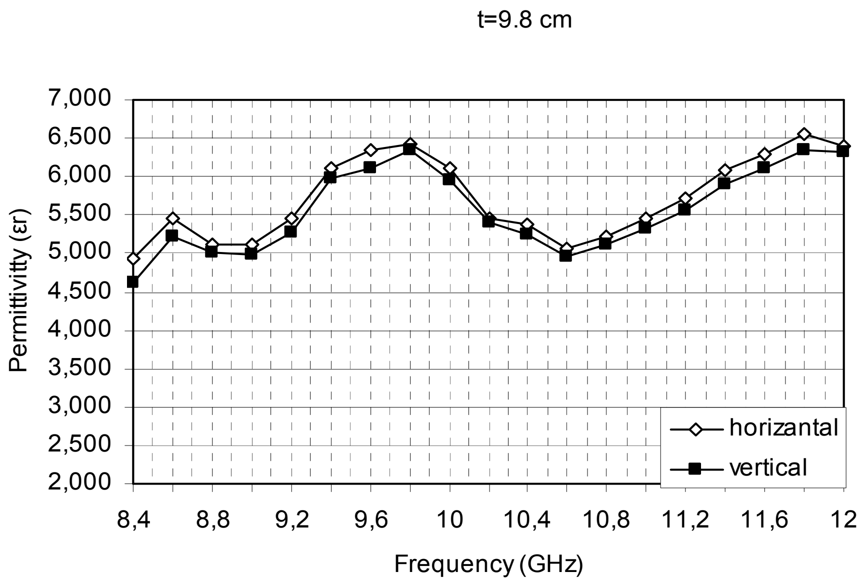

Figure A.5. Plot of permittivity for 9.8x15x15 cm and w/c:0.4 at different polarizations.

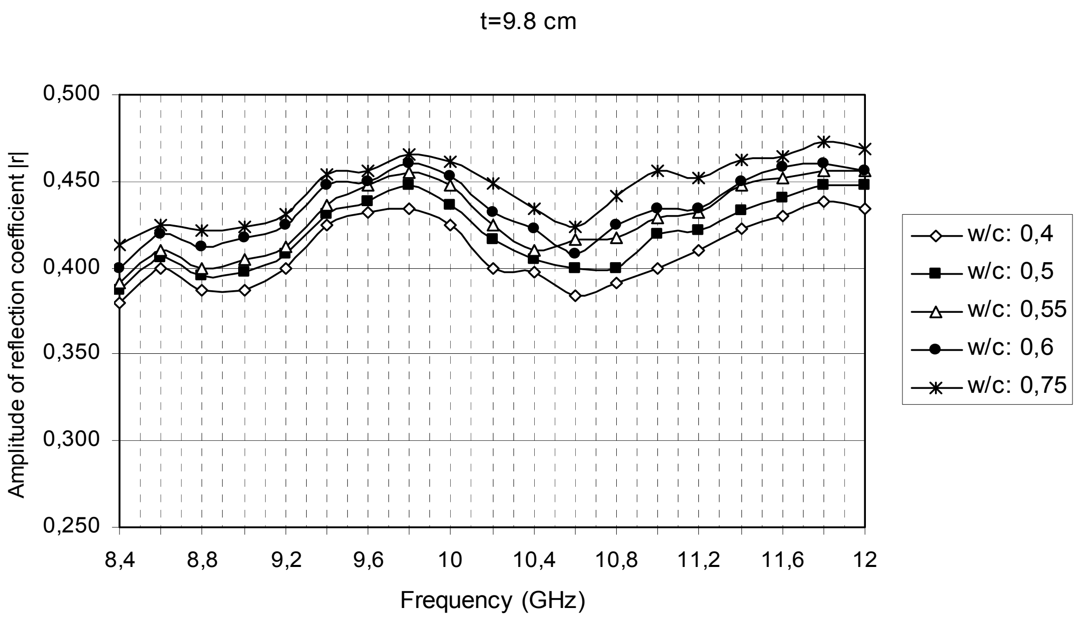

Figure A.6. Plot of comparison reflection coefficients for dimensions 9.8x15x15cm, at different ratio of w/c and between 8.4 GHz and 12 GHz at horizontal polarization.

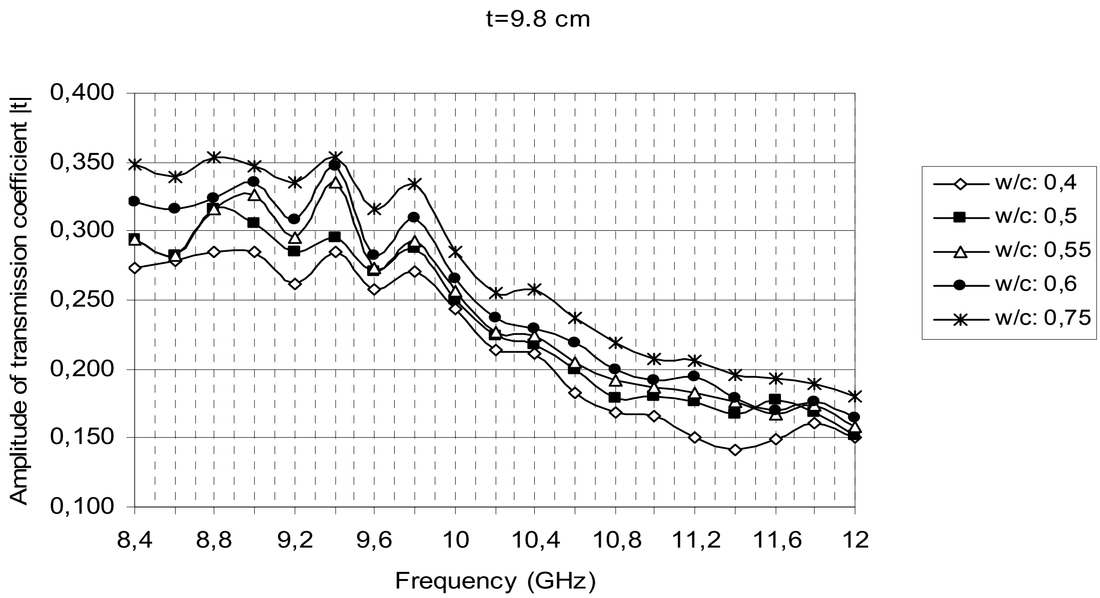

Figure A.7. Plot of comparison transmission coefficients for dimensions 9.8x15x15 cm, at different ratios of w/c, between 8.4 GHz and 12 GHz and horizontal polarization.

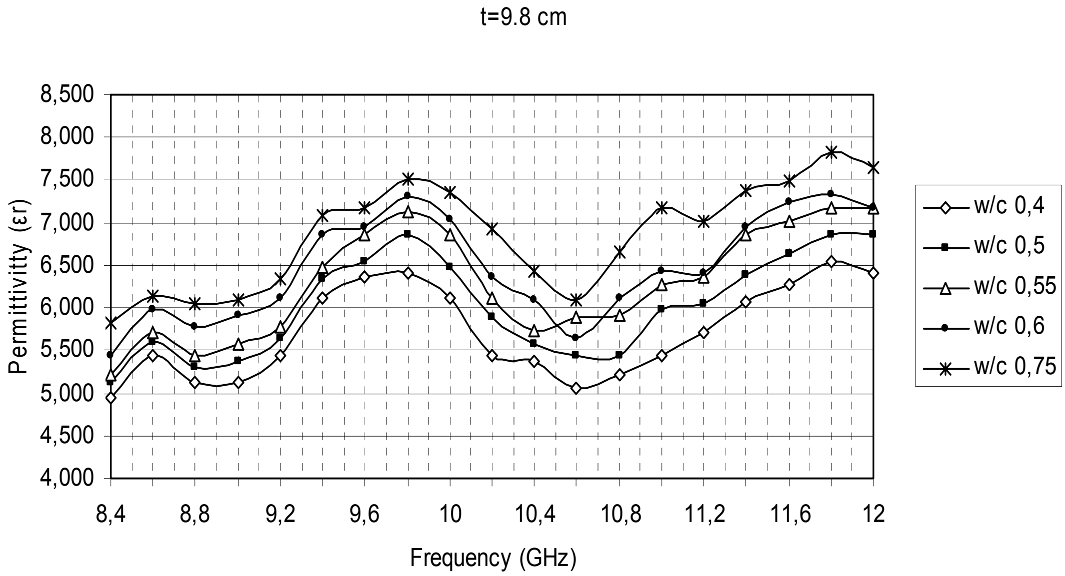

Figure A.8. Plot of comparison permittivity for dimensions 9.8x15x15 cm at different ratios of w/c, between 8.4 GHz and 12 GHz and at horizontal polarization.

In Figure A.6., A.7 and A.8. the curves correspond to the amplitude variation of the reflection, transmission coefficients and permittivity for the 9.8x15x15 cm specimens which have different w/c. Results show that when ratio of w/c increases, amplitude of reflection and transmission coefficients increase, too. Also, they show the variation of amplitude of these coefficients with frequency and it is seen that while the transmission coefficient decreases with frequency, reflection coefficient and permittivity increases with frequency.

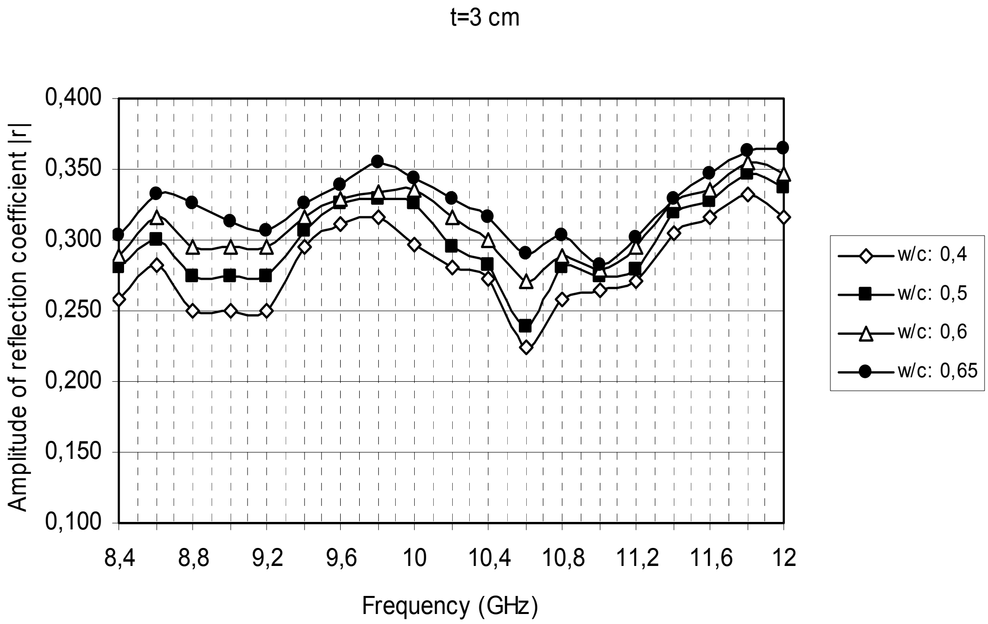

Figure A.9. Plot of comparison reflection coefficients for dimensions 3x15x15 cm, at different ratios of w/c, between 8.4 GHz and 12 GHz and at horizontal polarization.

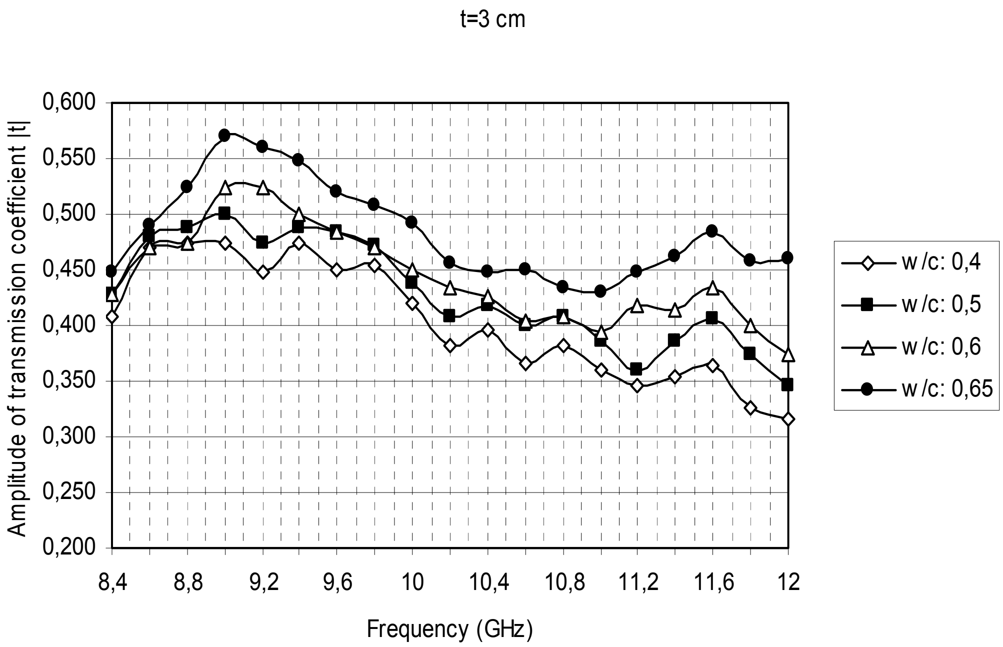

Figure A.10. Plot of comparison transmission coefficients for dimensions 3x15x15cm, at different ratios of w/c, between 8.4 GHz and 12 GHz and at horizontal polarization.

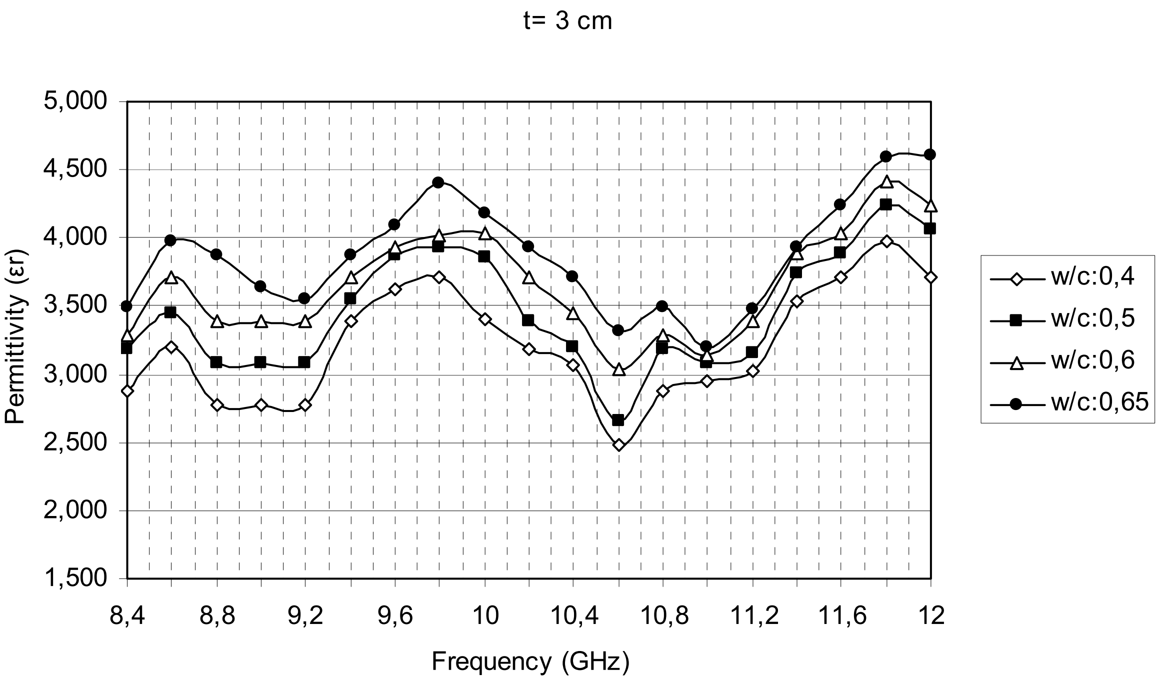

Figure A.11. Plot of comparison permittivity for dimensions 3x15x15 cm, at different ratios of w/c, between 8.4 GHz and 12 GHz and at horizontal polarization.

In Figure A.9, A.10 and A.11, for the 3x15x15 cm specimen's curve correspond to the amplitude of reflection, transmission coefficients and permittivity for different w/c. Again, when w/c increases, amplitude of reflection, transmission coefficients and permittivity increase, too.

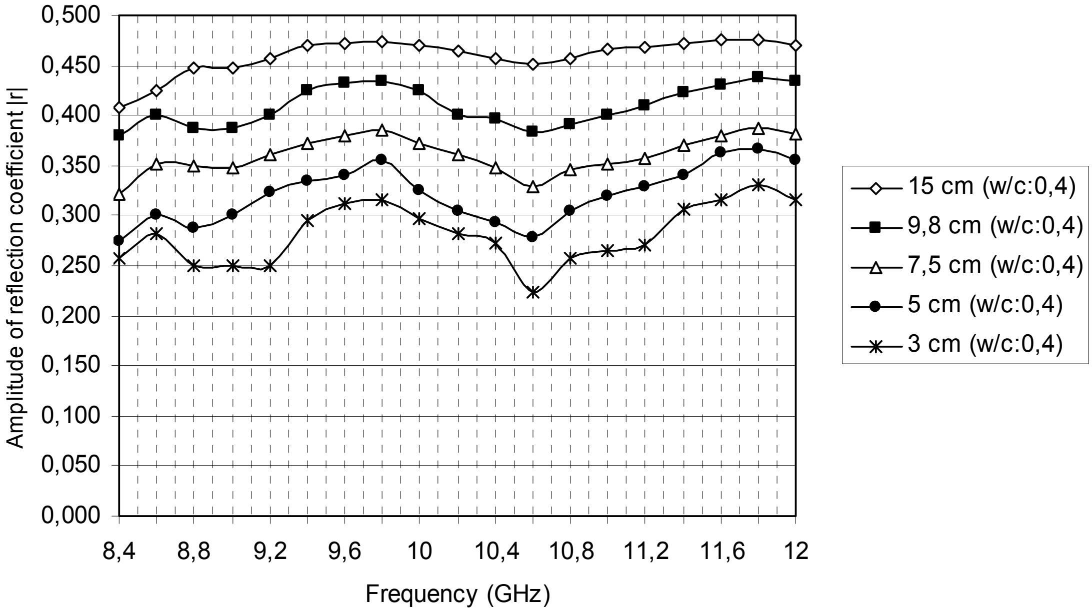

Figure A.12. Reflection coefficient for different thickness but same w/c:0.4 at between 8.4 GHz and 12 GHz and at horizontal polarization.

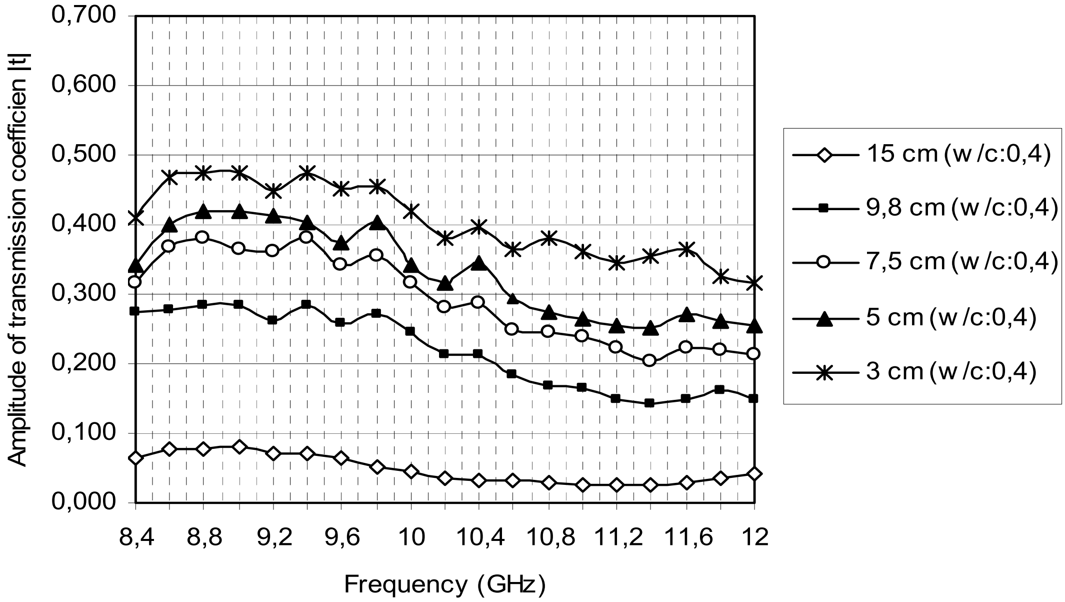

Figure A.13. Transmission coefficient for different thickness but same w/c:0.4 between 8.4 GHz and 12 GHz and at horizontal polarization.

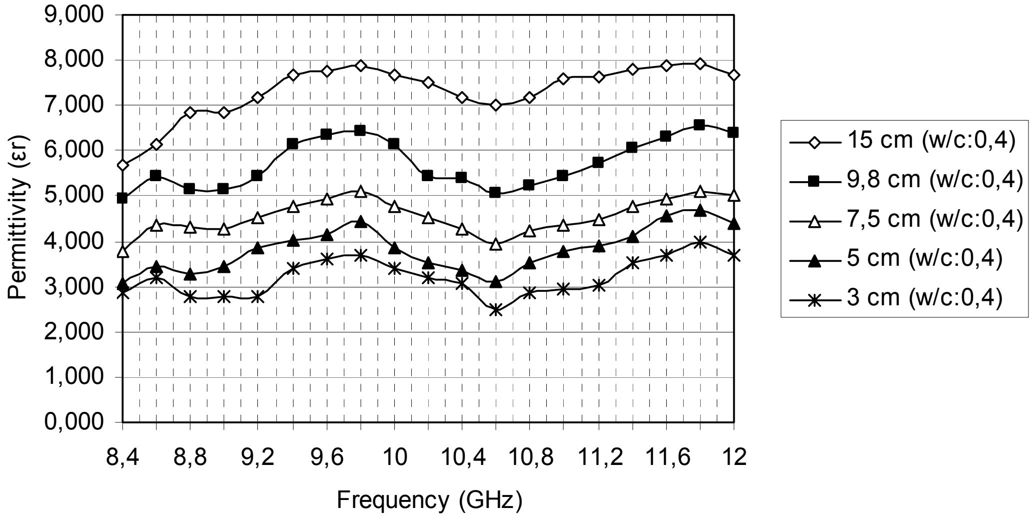

Figure A.14. Permittivity for different thickness but same w/c:0.4 between 8.4 GHz and 12 GHz and at horizontal polarization.

In Figure A.12., A.13 and A.14., the curves correspond to amplitude of the reflection and transmission coefficients and permittivity with different thickness but at same w/c. In Figure A.12. and A.14 amplitude of reflection coefficient and permittivity increase with thickness, but in Figure A.13. amplitude of transmission coefficient decrease with increasing w/c. Actually, these results are expected because, the transmission coefficient decrease with thickness of structure.

4-) Formulation of Dielectric Properties

Now, the data obtained by measurements are used to derive mathematical expressions for the reflection, transmission coefficient and permittivity by using the version of Matlab 7.0. with Curve Fitting Toolbox. The calculation was realized using the version of MATLAB 7.0. *cftool* command.

For according to results of measured in Figure A.12., A.13 and A.14., formulations of the reflection, transmission coefficients and permittivity which depend on frequencies and thickness are as following;

R(f,t)=(-0.008238).f^8+(0.6868).f^7-(24.99).f^6+(518.5).f^5-(6708).f^4+(5.54e+004).f^3-(2.853e+005).f^2+(8.371e+005).f-(1.072e+006) - (4.557e-005).t^4+(0.001435).t^3-(0.01553).t^2+(0.08585).t- (0.1529)

T(f,t)=(0.0009938).f^5-(0.05372).f^4+(1.162).f^3-(12.55).f^2+(67.6).f-(145)+(0.0001305).t^4-(0.004505).t^3+(0.05282).t^2-(0.2733).t+(0.8107)

P(f,t)=(-0.1226).f^8+(10.18).f^7-(369.4).f^6+(7642).f^5-(9.856e+004).f^4+(8.118e+005).f^3-(4.168e+006).f^2+(1.22e+007).f-(1.559e+007)-(0.001189).t^4+(0.03708).t^3+ (-0.3805).t^2+ (1.853).t +(-3.038)

These formulas, give good agreements with measurements. Of course these formulas validate for samples which were done measurements. Also, formulas are detected with version of Matlab 7.0. using by *polyfit, polval* commands. The polyfit command is used to generate n*th* degree polynomial. The polyval command uses the coefficients generated from polyfit to find.

The comparisons show that identities between formula and measurements, for the reflection, transmission coefficients and permittivity.

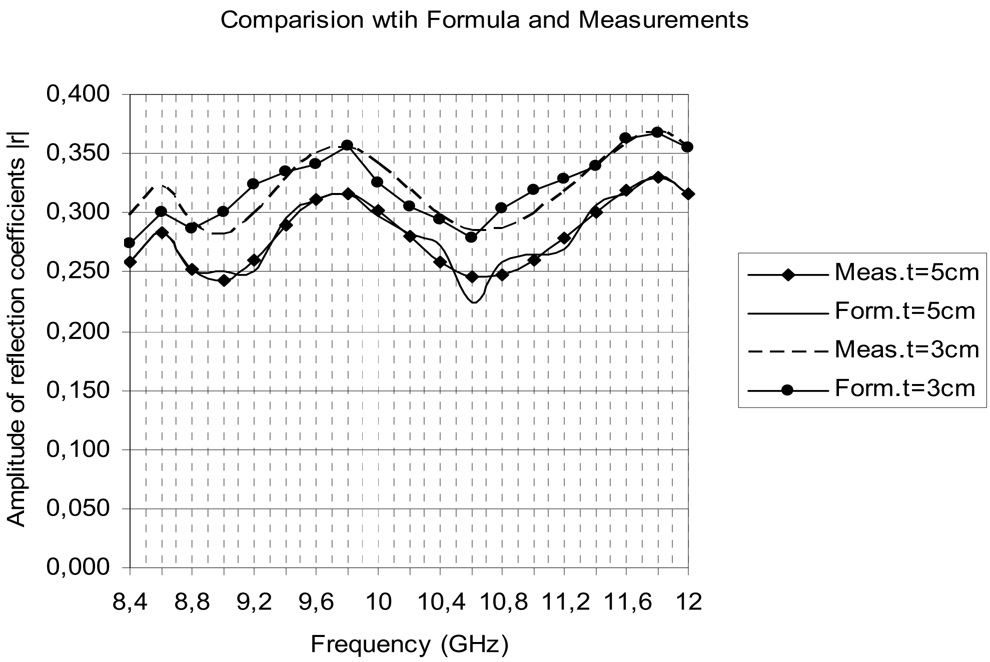

Figure A.15. Plot of formula and measured results for thickness of 5 and 3 cm.

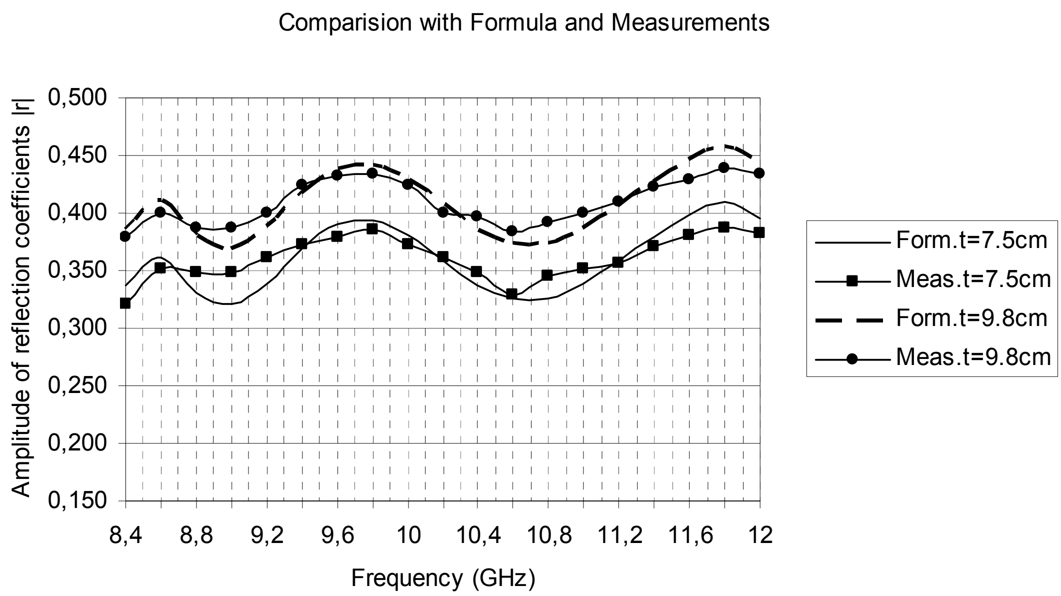

Figure A.16. Plot of formula and measured results for thickness of 7.5 cm and 9.8 cm..

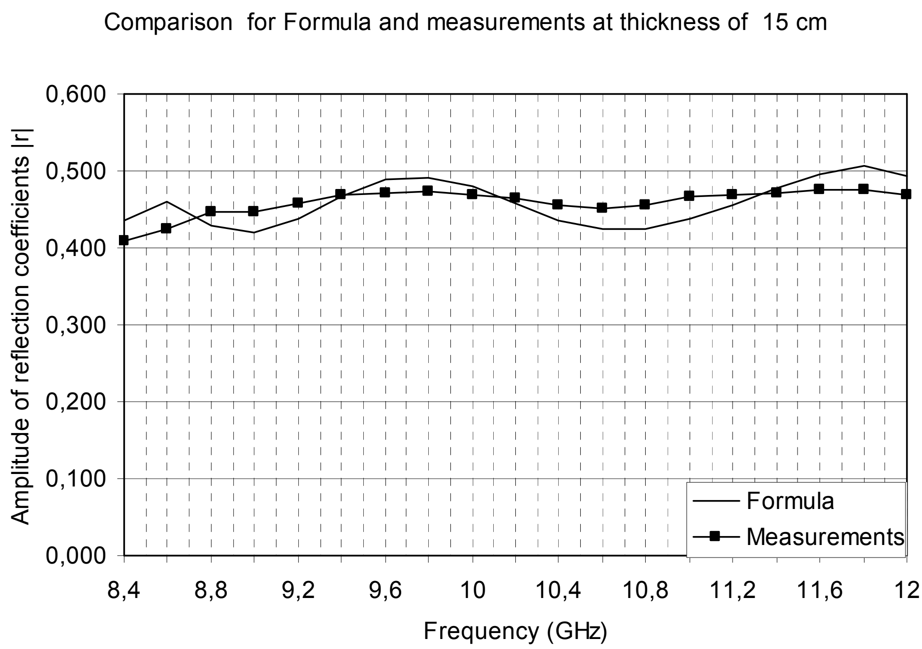

Figure A.17. Plot of formula and measured results for thickness of 15 cm.

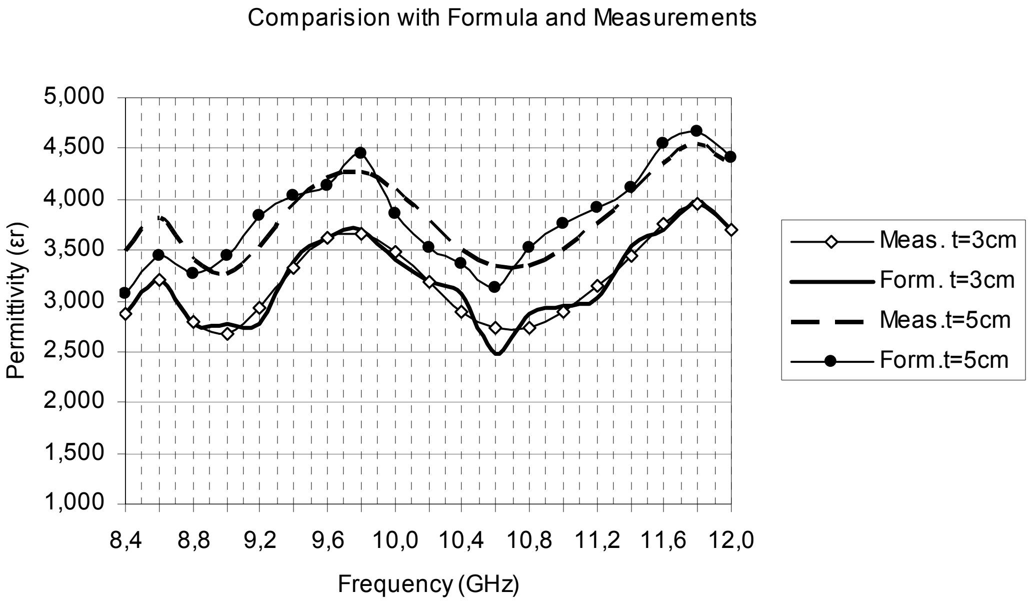

Figure A.18. Plot of formula and measured results for thickness of 3 cm and 5 cm.

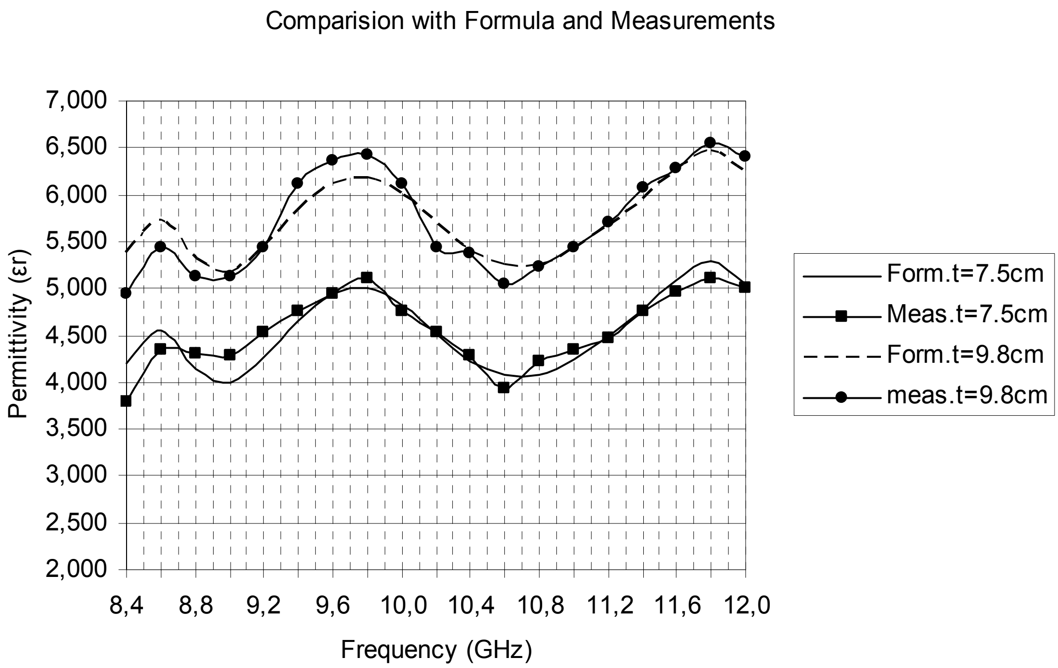

Figure A.19. Plot of formula and measured results for thickness of 7.5 cm9.8 cm.

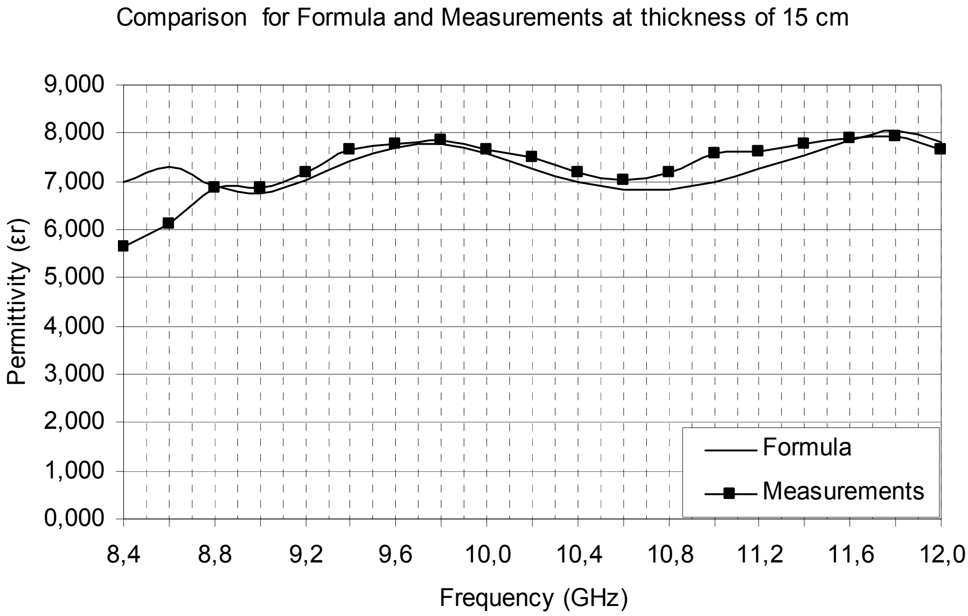

Figure A.20. Plot of formula and measured results for thickness of 15 cm.

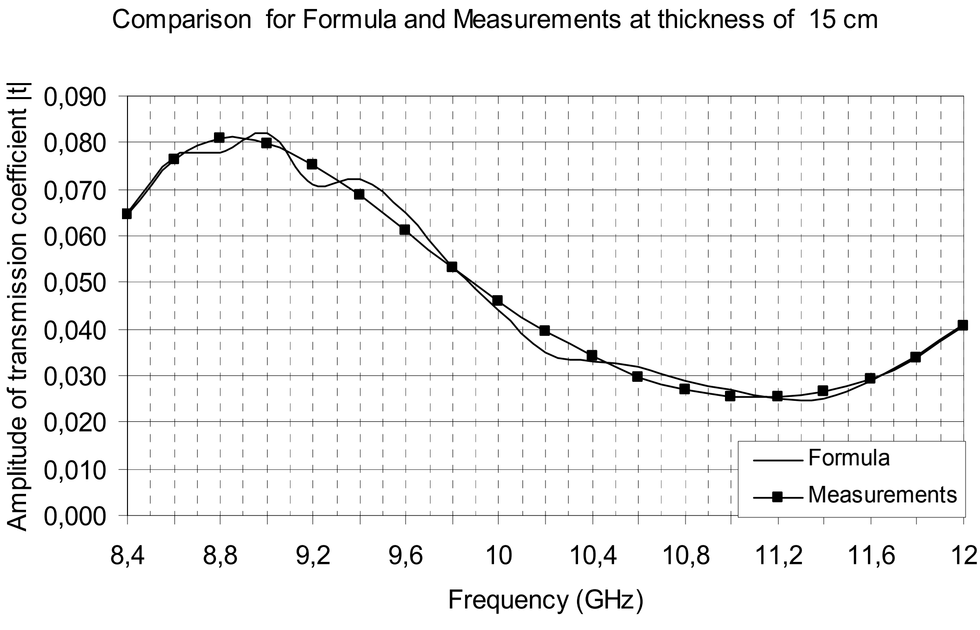

Figure A.21. Plot of formula and measured results for thickness of 15 cm.

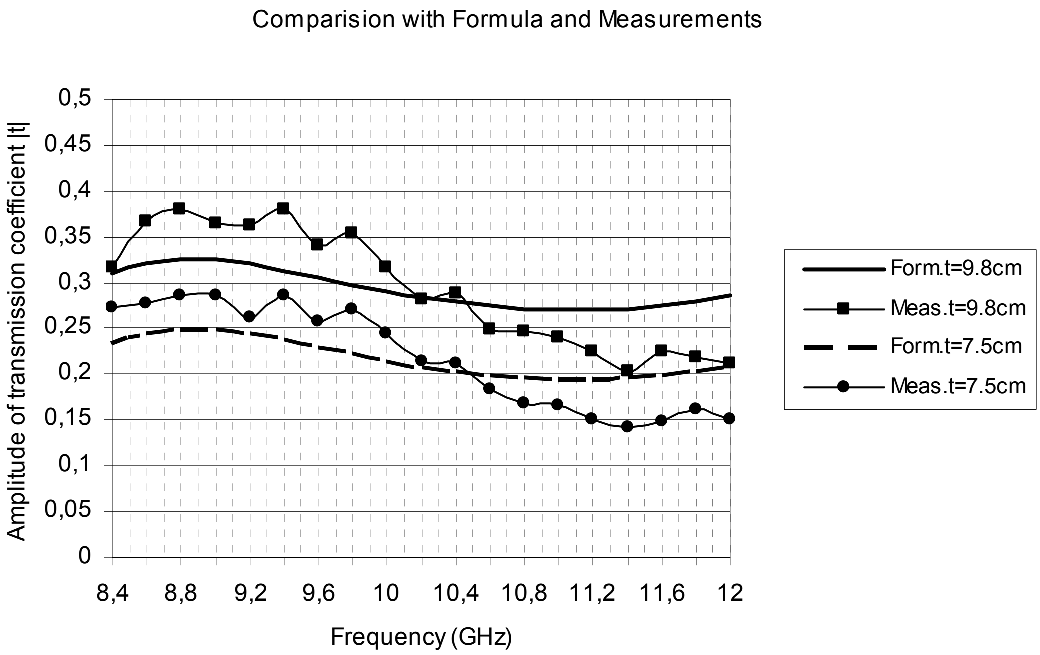

Figure A.22. Plot of formula and measured results for thickness of 9.8 cm 7.5 cm.

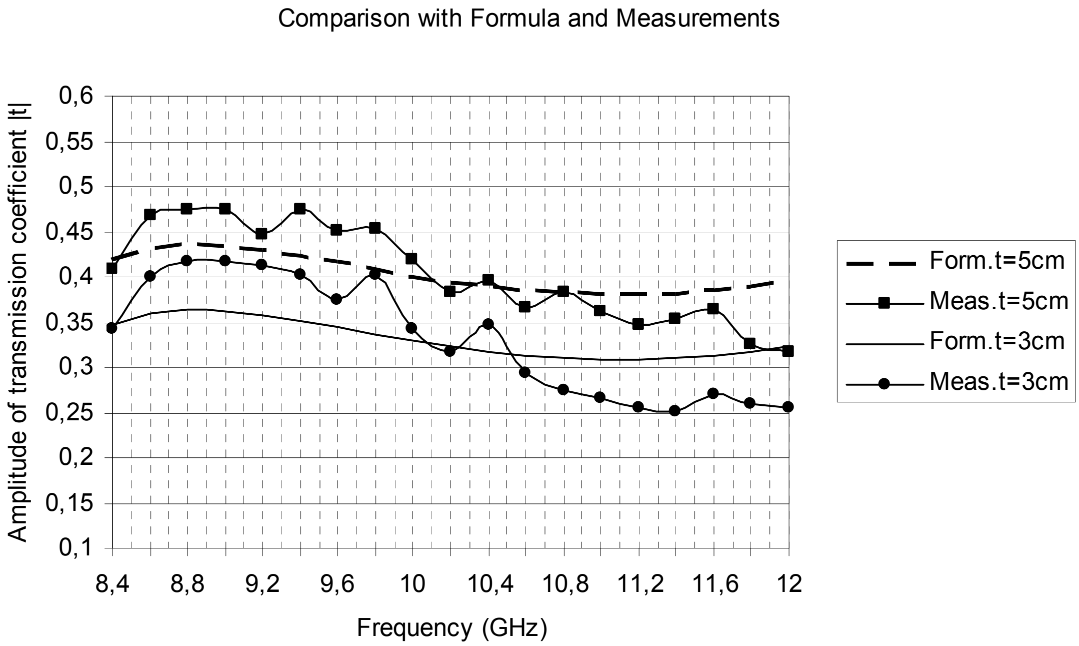

Figure I.23. Plot of formula and measured results for thickness of 5 cm and3 cm.

Results show that formulas and measurement very compatible each other. This is a quick and easy calculation which allows for an evaluation of the fitting procedure. In general, the error will continue to drop as the degree of polynomial is increased. This is because every extra degree of freedom allows for a better least-squares fit to data.